Structural Homology and Dynamic Variation in a Series of Porphyrin Bipyridinium Receptors and Their [2]Catenanes

Maxwell J. Gunter,*[a] Tyrone P. Jeynes,[a] and Peter Turner[b]

Keywords: Porphyrins / Catenanes / Dynamics / Bipyridinium / Receptors

We describe the successful synthesis of the porphyrin [2]catenanes, which completes a set of six structures where the length of the polyethylene glycol strap over the porphyrin is regularly increased from diethylene to triethylene to tetraethylene, and the central electron-donor component is either hydroquinol- or naphthoquinol-based. In the synthetic route to the strapped porphyrin precursors, co-formation of "straight" and "twisted" atropisomers in the longer strapped derivatives, and dimeric and higher oligomeric structures for the shorter straps, has been observed. Catenation results in only a single [2]catenane in each case. X-ray crystal structures of two representative strapped porphyrins are described. For each of the untwisted singly-strapped porphyrins, there is significant binding of paraquat within the cavity formed by the strap, and the binding constants range over about two orders of magnitude. For the catenanes, in each case the overall structural motif is similar to that previously observed for related members of the series. The temperature-dependent dynamic properties of the catenanes have been examined by ^{1}H NMR methods, and the rates of rotation increase from 50 to 25 000 to 340 000 s^{-1} at room temperature as the length of the strap increases by one ethylene glycol unit on each side. For the similarly sized naphthoquinol derivatives, the rotation rates are reduced by many orders of magnitude, ranging from essentially zero to 10 to 100 times per second at 25 °C through the same increase in chain length as for the hydroquinol analogues. The rates for a second process described as "out, turn around and in again", range from 2 to 400 to 110 000 s^{-1} at 25 °C in this naphthoquinol porphyrin series. The electronic spectra of the catenanes themselves do not show any significantly enhanced charge-transfer bands over the hydroquinol counterparts.

Introduction

The use of a catenane as a component of a molecular device,[1] or a molecular-scale machine[2,3] requires the ability to exercise precise control over its dynamics and chemistry by such external stimuli as protonation, electrochemistry, or photochemistry. In these cases, the catenane is required to have an in-built addressable component.[3,4] Porphyrins are excellent candidates for this, as they provide a particularly useful range of controlled functionality that can be accessed through chemical, electrochemical, or photochemical means, and there have been several examples where they are incorporated into catenated structures.[5–9]

Previously, we embarked on a program to synthesise a complete series of porphyrin hosts which are capable of complexing paraquat in a manner analogous to the [bis-(*p*-phenylene)-(3*n* +4)-crown-*n*] or [bis-(1,5-dinaphtho)-(3*n* +8)-crown-*n*] ethers. Since π-stacking interactions are a fundamental requirement in paraquat complexation and catenane synthesis, we reasoned that by replacing one of the electron-rich hydroquinol- or naphthoquinol- components of the crown ether with a large extended π-electron-rich porphyrin ring, we should be able not only to enhance paraquat complexation, but also facilitate catenane formation. Indeed with a hydroquinol- or naphthoquinol-ring centrally located within a polyether chain over-arching the porphyrin, we have shown that these porphyrin hosts complex paraquat, a concept which subsequently has led to the self-assembly of the corresponding porphyrinic [2]catenanes.

The strategy for catenane self-assembly was based on that employed by Stoddart and co-workers for analogous non-porphyrinic assemblies. Thus we synthesised a number of strapped porphyrins **1a** and their [2]catenanes **1c** and have examined in some detail the effects on their dynamics, chemical and photophysical behaviour.[7–10] Structural variations proved to have a profound influence on the observed dynamic behaviour of the catenanes synthesised thus far as evidenced by the wide range in the calculated thermodynamic parameters for the diethylene to triethylene series of strapped porphyrin catenanes.

[a] Chemistry, School of Biological and Biomedical Sciences, University of New England,
Armidale, NSW 2351, Australia
Fax: (internat.) + 612-6773-3268
E-mail: mgunter@metz.une.edu.au
[b] School of Chemistry, University of Sydney,
Sydney, NSW 2006, Australia
Supporting information for this article is available on the WWW under http://www.eurjoc.org or from the author.

 DOI: 10.1002/ejoc.200300493

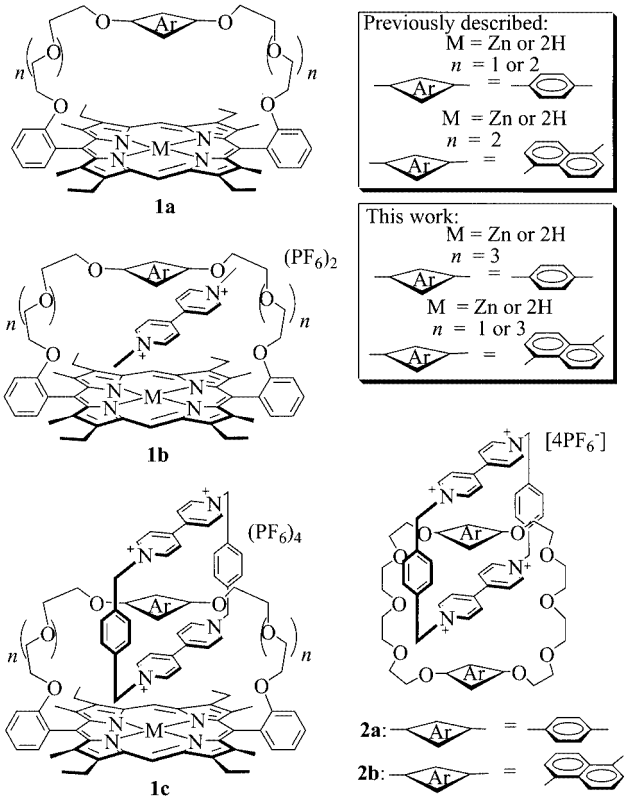

With this set of catenanes in hand, our next aim was to delineate the structure-activity profile of these intriguing porphyrin catenanes by probing their behaviour under a range of stimuli, including chemical (acid/base), redox, and photochemical studies[6,11,12] as both the length of the overarching strap, and the central electron-rich unit were varied. We have previously described the synthesis, solution state, and in some instances solid-state properties, bipyridinium binding behaviour, and [2]catenanes for the members of the series **1a**−**c:** n = 1 and 2, Ar = phenyl; and **1a**−**c:** n = 2, Ar = naphthyl.[8,9,13] For a more rational assessment of these factors, we now report the remaining three members of this series, **1a**−**c:** n = 3, Ar = phenyl; and **1a**−**c:** n = 1 and 2, Ar = naphthyl, which completes a set of porphyrin catenanes where two factors are varied systematically − the chain length of the strap and the nature of the central π-donor unit (hydroquinol or naphthoquinol). In completion of this series, we have encountered some new structural types involving atropisomers and oligomers, and these are also described.

We are now in a position to provide a complete catalogue of their fundamental properties, to allow a more systematic and rational structure-activity relationship within the series.

Results and Discussion

Porphyrin Synthesis and Solution Structures

The synthesis of the hydroquinol- and naphthoquinol-containing crown ether-strapped porphyrins **1a** (n = 3; Ar = phenyl) and **1a** (n = 1 and 3; Ar = naphthyl) is outlined in Schemes 1 and 2 and follows a similar methodology to that employed for the synthesis of the previously reported tri- and diethylene glycol-strapped analogues.[8] The dialdehyde strap precursor **4** was condensed with the dipyrrylmethane **5** using acid catalysis; trifluoroacetic acid with Cs_2CO_3 [14] in methanol for **6** and **7**, *p*-toluenesulfonic acid in the case of **8** and **9**, and trifluoroacetic acid for **10**, followed in each case by oxidation of the porphyrinogen with *o*-chloranil to give the desired porphyrin products which were then separated by column (silica) chromatography.

In the case of the two longer strapped derivatives (n = 3), two atropisomers **6** and **7**; and **8** and **9**, were isolated in each case (Scheme 1). These were identified on the basis of NMR spectral evidence, as the "twisted" or α,β-isomer, and the "over-the-top" α,α-isomer respectively. This type of isomerism has been previously reported by us, and others, and it appears to be commonly observed for porphyrins strapped by long chains.[13,15,16]

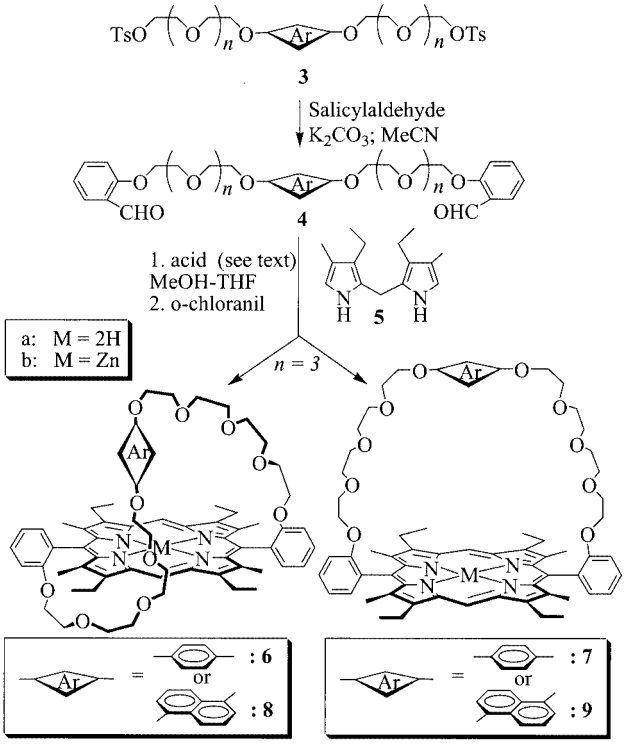

Scheme 1

Several pieces of evidence confirm the atropisomeric relationship between **6** and **7**, and **8** and **9**. Firstly, the pairs of isomers have the same pattern in their electrospray mass spectra with peaks observed for the parent ion (singly and doubly charged). Secondly, the ^{1}H NMR resonance of the hydroquinol (HQ) ring protons at δ = 6.91 ppm in the "twisted" strapped porphyrin isomer **6a** are shifted significantly downfield (deshielded +0.78 ppm) compared to

Table 1. Selected ^{1}H NMR spectroscopic data for the hydroquinol- and naphthoquinol-strapped free base and zinc porphyrins and their isomers at 300 MHz in $CDCl_3$ at 298 K

Position	**6a**	**7a**	**9a**	**9b**	**8a**	**8b**[a]	**10a**	**10b**
meso-H	10.10	10.17	10.18	10.12	10.02	10.02	10.14	9.92
porph. CH_2CH_3	3.93	4.00	4.00	3.99	3.80	3.87	3.98	3.94
porph. CH_2CH_3	1.69	1.78	1.78	1.77	1.58	1.65	1.75	1.77
porph. CH_3	2.50	2.55	2.56	2.52	2.42	2.39	2.57	2.52
Pyrrole NH	−2.42	2.37	−2.33	–	−2.47	–	–	–
meso-φ *o*-	7.73	7.65	7.61	7.74	7.69	7.58	7.69	7.73
meso-φ *m*-	7.32	7.31	7.29	7.27	7.26	7.19	7.34	7.34
meso-φ *p*-	7.74	7.74	7.73	7.73	7.71	7.69	7.74	7.76
meso-φ *m′*-	7.34	7.33	7.31	7.28	7.31	7.34	7.32	7.28
OCH_2 H-1[b]	4.14	4.16	4.08	4.02	4.11	4.12	4.28	4.11
OCH_2 H-2[b]	3.18	3.15	3.05	2.84	3.15	3.18	3.47	3.04
OCH_2 H-3[b]	2.28	2.53	2.47	1.99	2.25	2.39	3.20	2.33
OCH_2 H-4[b]	2.19	2.49	2.54	1.99	2.16	2.31	2.82	1.88
OCH_2 H-5[b]	2.67	2.64	2.70	2.67	2.75	2.52	–	–
OCH_2 H-6[b]	3.01	2.64	2.70	2.67	3.18	2.81	–	–
OCH_2 H-7[b]	3.44	2.80	2.91	2.67	3.70	3.34	–	–
OCH_2 H-8[b]	3.93	3.15	3.23	2.91	4.23	3.85	–	–
HQ	6.91	6.13	–	–	–	–	–	–
NQ(α)	–	–	5.88	6.03	6.86	6.76	3.77	3.79
NQ(β)	–	–	6.74	6.90	7.41	7.39	4.11	5.17
NQ(γ)	–	–	7.37	7.34	7.95	7.80	6.24	6.39

[a] Recorded at 303 K. [b] Numbering H-1 to H-8 refers to OCH_2 protons commencing at the *meso*-aryl ring, and increasing to the central naphthoquinol or hydroquinol ring of the strap.

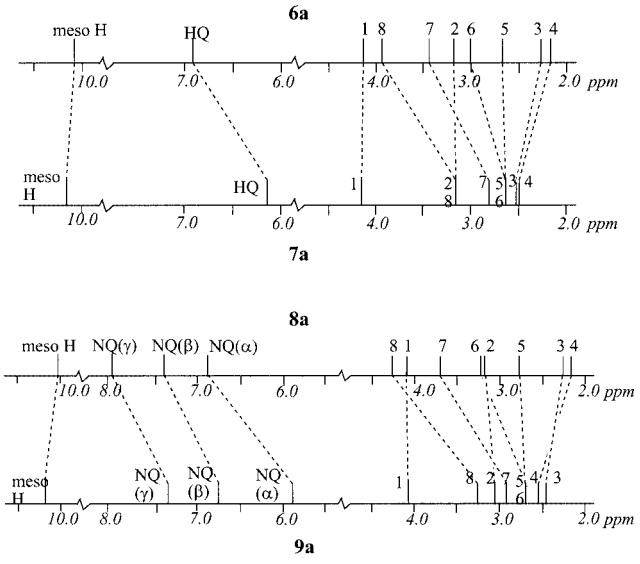

Figure 1. Schematic representation of the differences in the chemical shifts of the "twisted"- or α,β-strapped porphyrins **6a** and **8a** compared to their α,α-atropisomers **7a** and **9a**. Numbering is as indicated in Table 1

those in **7a** at δ = 6.13 ppm (Table 1 and Figure 1). Similar trends were also observed for the zinc derivatives **6b** and **7b**. Also, the *meso* proton (*meso*-H) chemical shift at δ = 10.10 ppm in **6a** is shielded (Δδ = −0.07) in the ^{1}H NMR spectrum compared to that in **7a**. These chemical shift differences, represented schematically in Figure 1 imply that the HQ ring is held at the side of the porphyrin ring in **6a** and hence the HQ protons are deshielded by the porphyrin ring current, while the *meso*-H proton is shielded by the presence of the aromatic HQ ring, which is presumably held edge-to-face with the porphyrin ring. Furthermore, the chemical shifts of the methylene protons of the polyether strap in **6a** span a wider range compared to the α,α-isomer **7a**. For example the protons H-7 and H-8 (Table 1) are shifted significantly downfield in the α,β-isomer **6a** (Δδ +0.64 and +0.78, respectively) compared to **7a**, indicative of deshielding as a result of twisting around the side of the porphyrin. In contrast, the protons H-3 and H-4 are shifted upfield in the isomer **6a** compared to **7a** (Δδ −0.25 and −0.30 respectively) since these protons would be shielded by the porphyrin as a result of being held closer to the porphyrin macrocycle as the strap twists from one face to the other. Similar trends are also observed for the naphthoquinol analogues **8** and **9**, and the comparative shifts are also shown in Figure 1.

Similar trends were also noted for the zinc derivatives (**b**, Table 1), with some notable exceptions. For example the H-3 and H-4 protons of the polyether strap in the twisted isomer **8b** are *deshielded* (Δδ +0.40 and +0.32) compared to its zinc isomer **9b**, whereas the corresponding protons in the free base derivatives are *shielded* (Δδ = −0.22 and −0.38). Also the deshielding of the methylene strap protons closest to the *meso*-phenyl rings in **8b** compared to **9b** is greater than those of the corresponding free base derivatives, **8a** and **9a**, while those closest to the NQ ring in the zinc derivative are more shielded. This is consistent with the polyether chain of the zinc derivative in **9b** being folded in over the face of the same or a second porphyrin moiety (similar to the crystal structure of **9b** in Figure 3 − see below) and being shielded by the porphyrin, whereas on forming the zinc twisted isomer **8b**, the protons H-1 and H-2 are further deshielded, while H-3 and H-4 are now deshielded as a result of movement away from the porphyrin.

It was surprising that there was no apparent splitting of the porphyrin resonances, particularly for the *meso*-H, HQ, methyl and ethyl side-chain protons as a result of the apparent asymmetry in structures **6** and **8**. However, an examination of molecular models revealed that the polyether strap is long and flexible enough to allow facile interconversion of conformers which maintains equivalence of the porphyrin protons.[17] Even down to 220 K, no asymmetric splitting was observed, although the HQ protons in **6a** and **8a** did broaden considerably, whereas the HQ and NQ ring protons in **7a** and **9a** remained sharp at this temperature.

Nevertheless, interconversion of **6** and **7**, and of **8** and **9**, by free rotation of the *meso*-phenyl ring around the C9−10 axis can be observed readily: solutions of pure samples of either **6a** or **7a** were found to reach an equilibrium mixture of approximately 12:88 at room temperature over 30 days, when monitored by either TLC or ^{1}H NMR spectroscopy. Alternatively, this equilibration process was complete within one hour in refluxing acetonitrile solution. Likewise for the naphthoquinol analogues **8b** and **9b**, equilibration was complete (8:92) after 30 days at room temperature, or 3 h in refluxing acetonitrile.

The synthesis of the "tighter" naphthoquinol-strapped porphyrin **10** resulted in the formation of several oligomeric and isomeric porphyrins in significant quantities, in addition to the monomeric, single-strapped derivative **10** (Scheme 2). The oligomeric nature of these were proven by MS in the first instance, which showed that monomeric **10**, dimeric and atropisomeric **11** and **12**, and trimeric porphyrin products had been isolated from the reaction. In the electrospray mass spectrum of the monomeric **10b** only one parent ion peak was seen at 1025.8 (calcd. 1025.4), whereas the dimeric **11b** and **12b** produced a very large peak in the FAB-mass spectrum at 2051.9 (calcd. 2052.85) as well as a monomer peak at 1026.4 (calcd. 1026.43), whereas the FAB-MS for the trimeric species had peaks with the same mass values as **10b** and **11b/12b** as well as a peak (with the same intensity as the monomeric peak) at 3078.24 (calcd. 3079.28) corresponding to a porphyrin trimer.

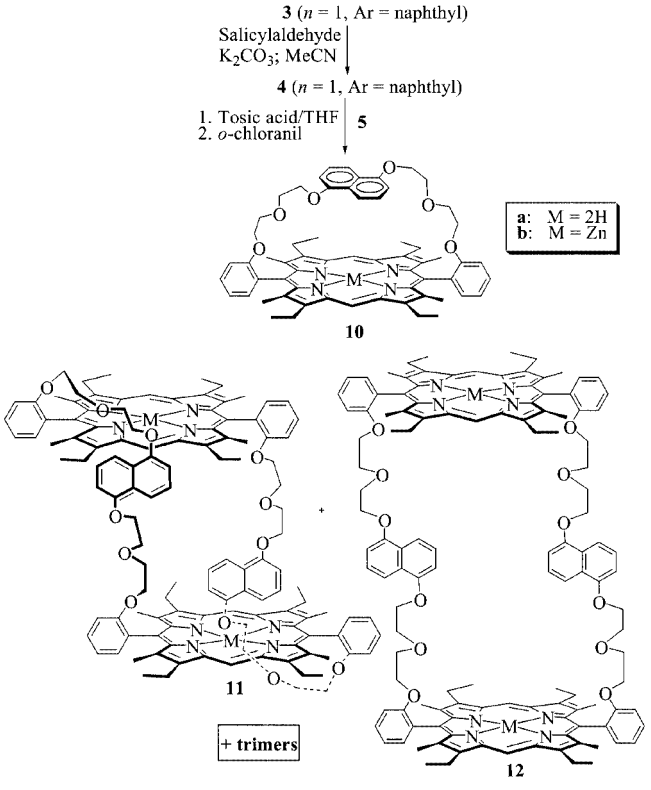

Scheme 2

Assignment of the ^{1}H NMR resonances for both the free base **10a** and zinc **10b** monomeric strapped porphyrin derivatives are shown in Table 1. The shifts of the relevant resonances for the strap and the porphyrin are consistent with the strapped structure, as now a clear pattern has emerged across the range of strapped porphyrins both in this and other studies. The most significant aspect of the spectra of **10a** and **10b** are the large upfield (shielded) resonances for the naphthoquinol protons as a result of an enforced close proximity to the porphyrin face by the relatively short diethylene glycol chains, compared to the longer strapped analogues. A more detailed analysis of the NMR assignments for the dimeric **11** and **12** and trimeric species at both high and low temperatures, and aspects of their electronic spectra, are given in the supplementary material.

Solid-State Structures

Single crystal structures of **10b** and **7b** were determined by X-ray diffraction, and ORTEP[18] depictions are shown in Figure 2 and 3. A closely related analogue of **7b**, with a naphthoquinol unit linked across the face of the porphyrin by triethylene glycol chains rather than the tetraethylene glycol units of **7b**, has been reported previously.[13] Likewise a paraquat $\mathbf{PQ^{2+}}$ complex of **1:** $n = 2$, Ar = naphthyl has been described previously.[13]

The metal coordination geometry of the **10b** complex is square pyramidal with an apical dimethyl sulfoxide ligand bound within the porphyrin cavity. The metal to apical oxygen distance is typical at 2.125(1) Å. The pyrrole nitrogens of the metalloporphyrin are essentially co-planar, with no deviation greater than 0.006(2) Å. The metal ion is displaced 0.300(1) Å from this plane towards the axial ligand. The porphyrin strap appears to be responsible for the C(10) and C(20) *meso* carbons being 0.320(3) and 0.257(3) Å above the square pyramid basal plane, and the C(5) and C(15) atoms being correspondingly 0.288(3) and 0.324(3) Å below that plane. Adjacent pyrrole groups are accordingly slightly tilted towards each other, with respect to the basal plane. The strap of the inversion centre related neighbouring metalloporphyrin immediately above the complex is in van der Waals contact with the N(1) and N(2) pyrrole groups. The intruding strap is responsible for the metalloporphyrin strap being offset from the porphyrin centre and inclined at 26.80(3) ° with respect to the 24 atom porphyrin least-squares plane. The cavity bound dimethyl sulfoxide ligand prevents any intramolecular interaction between strap and porphyrin.

Surprisingly the **7b** metalloporphyrin forms discrete dimers in the solid state, such that the Zn of one porphyrin is coordinated by a polyether chain oxygen of an inversion related complex (Figure 4).[19] The coordination geometry is again square pyramidal, with the metal to ether oxygen distance being 2.257(5) Å. In contrast to **10b** the porphyrin ring is essentially planar, with no deviation from the 24 atom least-squares plane greater than 0.078(9) Å, and the pyrrole nitrogens deviate no more than 0.011(8) Å from the equatorial coordination least-squares plane. The metal ion is drawn 0.209(1) Å from the core least-squares plane towards the coordinating polyether oxygen. Accommodating the coordinating neighbour, the polyether strap of **10b** is folded away from the porphyrin core, with the closest distance between the phenyl chain residue and the ring centre being approximately 8.7 Å. The phenyl residue in the strap forms a dihedral angle of 50.2(3) ° with the 24 atom porphyrin least-squares plane, and clearly there is no possibility for any intramolecular interaction between strap and porphyrin.

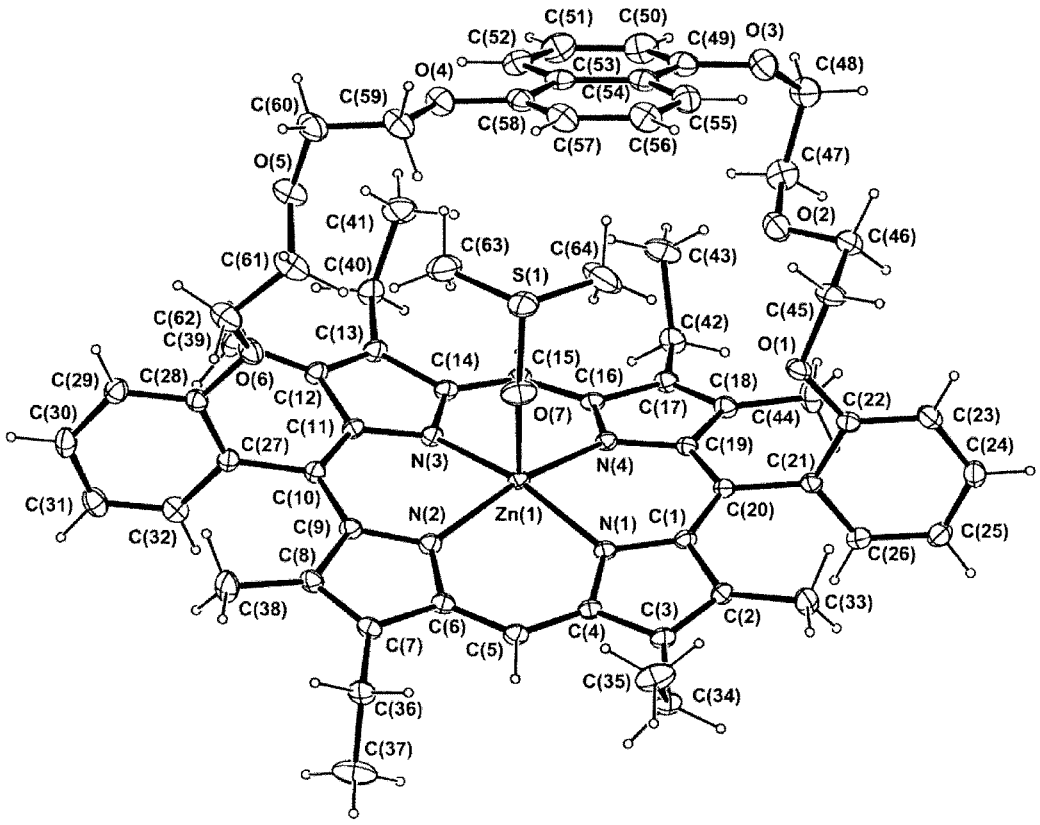

Figure 2. An ORTEP depiction, with 50 % displacement ellipsoids, of the naphthoquinol-containing diethylene-strapped zincporphyrin **10b**

Strapped Porphyrins as Receptors for Paraquat

As a prelude to the synthesis of the porphyrin [2]catenanes, binding studies were carried out for this new series of strapped porphyrin receptors. Previous complexation studies with paraquat for the analogous hydroquinol and naphthoquinol strapped porphyrins had established that these porphyrin hosts complex paraquat in a manner analogous to that of BPP34C10, ie with an inclusion geometry in which the hydroquinol (or naphthoquinol), paraquat, and porphyrin rings are held in a co-parallel manner, as indicated by **1b**.[8,12,13] At the same time, we wished to compare the binding strengths of a series of di-, tri-, and tetraethylene-strapped porphyrins to gauge the effect of increasing the length of the strap on the binding constant. This would reflect the importance of π−π interactions as a stabilizing force in noncovalent interactions and in subsequent template-directed synthesis. In addition, we wished to determine the effect of solvent polarity on the strength of binding in these systems.

To this end, a series of complexation studies was carried out in [D_6]acetone/[D_6]DMSO (20 %)[20] on the hydroquinol-strapped porphyrin host **7b** and the naphthoquinol-strapped porphyrin hosts **9b** and **10b** as well as the previously reported naphthoquinol triethylene-strapped porphyrin **1a** (n = 2, Ar = naphthyl) whose association constant was previously determined in DMF by ^{1}H NMR titration. The NMR shifts of both host and guest on binding followed the same trend as observed previously,[8,12,13] indicating a similar binding geometry in each case.[21] The calculated association constants, K, determined by the direct ^{1}H NMR titration method in [D_6]acetone/[D_6]DMSO (20:80) are collected in Table 2, together with values reported previously for other members of the series.

These results show that binding of paraquat is strongest in the tight diethylene-strapped naphthoquinol porphyrin **10b**. As expected, the strength of binding in the naphthoquinol-strapped porphyrin series is weaker as the length of the strap increases (entropic effect). Furthermore, the replacement of a naphthoquinol unit for a hydroquinol in analogous length strapped porphyrins reduces the effectiveness of π−π interactions and this is reflected in an approximate order of magnitude decrease in the strength of binding.

Also, this series of complexation studies highlights the solvent effect in the strength of binding (compare rows 3 and 5 in Table 2), which generally decreases as the polarity of the solvent increases, as we have also found in related crowned porphyrins.[13,22]

Porphyrin [2]Catenanes

The synthetic methodology employed for the self-assembly of the [2]catenanes used a modification of Stoddart's clipping strategy, as we have described previously for related porphyrin catenanes, and is outlined in Scheme 3. In the

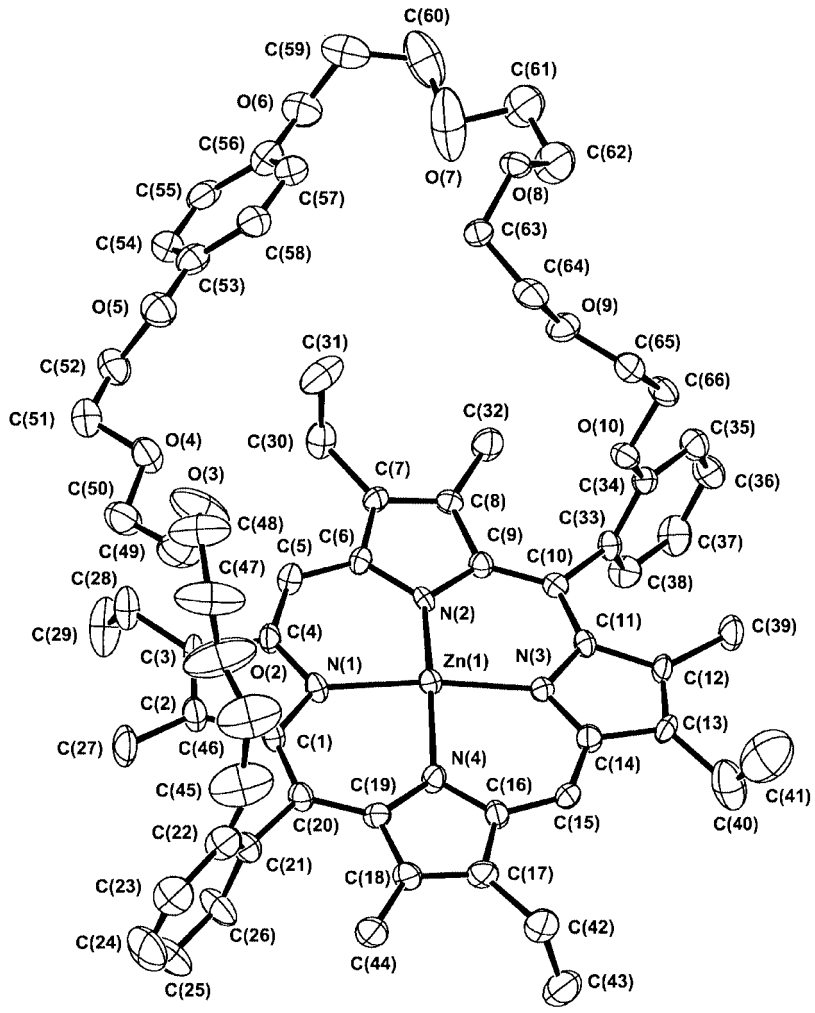

Figure 3. A labelled ORTEP[18] depiction, with 20 % displacement ellipsoids, of the hydroquinol-containing tetraethylene-strapped zincporphyrin **7b**. Axial coordination from an inversion related complex molecule is not shown (see Figure 4), and the hydrogen atoms have been removed for clarity

case of the longer (n = 3) strapped porphyrins (both hydroquinol and naphthoquinol), equilibrium mixtures of the atropisomeric **6b** (12 %) and **7b** (88 %), or the naphthoquinol-strapped porphyrin isomers **8b** (8 %) and **9b** (92 %), or the naphthoquinol-strapped porphyrin **10b** were used. In each case only a single catenane product was identified and isolated, indicating that atropisomersiation had occurred under the catenation conditions (12−14 days at 1 atm, or 3−4 days at 12 KBar pressure in DMF).[23]

Mass spectroscopic data were typical and diagnostic for catenanes of this type:[8,24] in FAB MS spectra, ion peaks for the stepwise loss of one to four counterions and the parent porphyrin were observed, with very few other fragment ions.

^{1}H NMR spectra for the porphyrin [2]catenanes were collected under conditions of either fast or slow exchange, with the exception of the diethylene-strapped naphthoquinol porphyrin [2]catenane **16** since the fast exchange limit could not be reached, indicating a large steric barrier for tetracation rotation in this tightly strapped catenane; instead this catenane decomposed above temperatures of about 380 K. The ^{1}H NMR resonances of the previously reported hydroquinol-strapped porphyrin [2]catenanes **1c**: n = 1, Ar = phenyl, and **1c**: n = 2, Ar = phenyl, as well as the naphthoquinol-strapped porphyrin [2]catenane **1c**: n = 2, Ar = naphthyl are included in Table 3. All previously reported catenanes show an increased chemical shift difference compared to the BPP34C10-based [2]catenane **2a**, due to the influence of the large magnetic anisotropy of the porphyrin macrocycle. However, the change in chemical shift for the hydroquinol ring proton (HQ) resonance upon catenane formation in **14** is very similar to the BPP34C10-based [2]catenane **2a**, which reflects the increased distance of the HQ ring away from the effects of porphyrin nucleus upon catenane formation. A similar effect is seen for the naphthyl derivative **15**.

As evidenced previously, these spectra support a structure in which the bipyridinium moiety, hydroquinol (or naphthoquinol) and porphyrin macrocycle are held co-parallel (see **1c** in Scheme 3) in a similar fashion to that shown for the complexation of paraquat: (i) the β-bipyridinium and α-bipyridinium protons ($\Delta\delta$ = −1.10 and −0.51) are

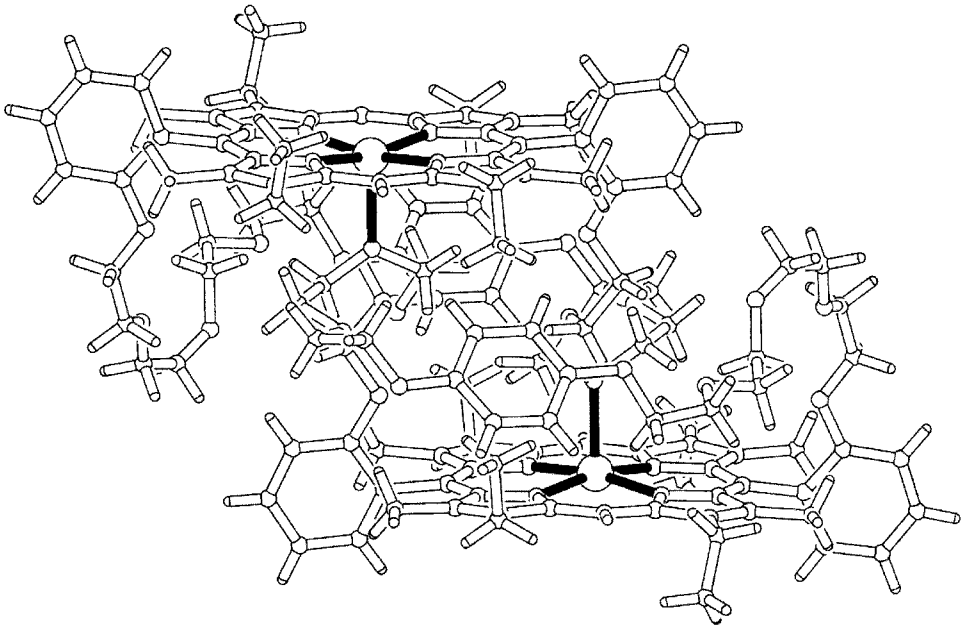

Figure 4. A "straw" depiction[19] of the strapped porphyrin **7b** showing the dimer formed by coordination of the O(8) ether oxygen of one porphyrin to the zinc atom of an inversion related metalloporphyrin

Table 2. Binding constants (K_a) for several hydroquinol and naphthoquinol containing crown-ether-strapped porphyrin hosts with paraquat determined by ^{1}H NMR titration in CD_3COCD_3/CD_3SOCD_3 (20 %) at 303 K

Host	K_a[a] (M^{-1})	$\Delta G°$ ($kJ \cdot mol^{-1}$)[b]
1a: n = 3, Ar = phenyl (**7b**)	3.1×10^2	−14.3
1a: n = 1, Ar = naphthyl (**10b**)	5.6×10^3	−21.5
1b: n = 2, Ar = naphthyl[c]	2.3×10^3	−19.3
1a: n = 3, Ar = naphthyl (**9b**)	1.0×10^3	−17.2
1b: n = 2, Ar = naphthyl[d]	2.1×10^4	−24.7

[a] Binding constants are averaged values from several protons monitored during the titration. [b] $\Delta G°$ values calculated from *Ka*. [c] K_a also measured in CH_3CN by fluorescence technique to be 1.0×10^4 M^{-1}. [d] Measured in [D_7]DMF at 298 K by ^{1}H NMR titration using a dilution method.

more affected by catenane formation then either the $^+NCH_2$ ($\Delta\delta$ = −0.86 and −0.42) or phenylene ($-C_6H_4-$) protons ($\Delta\delta$ = −0.33 and +0.11) which are least affected; (ii) under conditions of slow exchange, the β-bipyridinium resonances in the naphthoquinol porphyrin catenanes **16** and **15** are split into four peaks with a very large separation ($\Delta\delta$ = 3.77 and 3.74) for **16**; 3.38 and 4.36 ppm for **15**), which is significantly greater than the splitting observed for α-bipyridinium resonances ($\Delta\delta$ = 1.12 and 1.67 for **16**; 0.91 and 0.67 ppm for **15**) and the phenylene resonances ($\Delta\delta$ = 0.13 and 0.23 ppm for **16** and **15** respectively). This implies that the α- and β-bipyridyl protons of the bipyridinium moiety are held closest to the porphyrin, and thus most affected by the porphyrin magnetic anisotropy on catenane formation, and supports a structure in which the bipyridinium, hydroquinol (or naphthoquinol) and porphyrin units

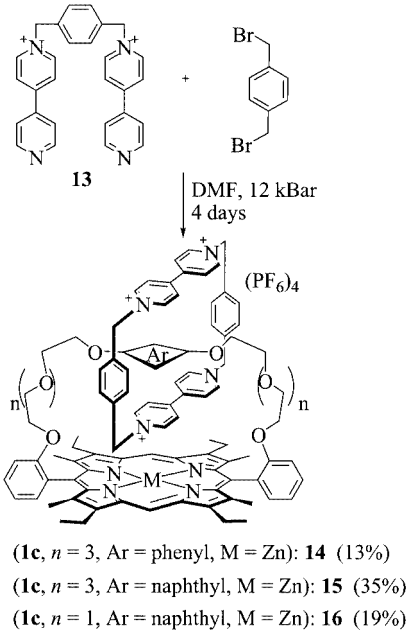

(**1c**, n = 3, Ar = phenyl, M = Zn): **14** (13%)
(**1c**, n = 3, Ar = naphthyl, M = Zn): **15** (35%)
(**1c**, n = 1, Ar = naphthyl, M = Zn): **16** (19%)

Scheme 3

are co-parallel (as in structures **1c**) rather than orthogonal, as described previously.[8]

The diastereotopicity that was observed within the methylene protons of the porphyrin periphery following paraquat complexation, is again seen in each of the porphyrin [2]catenane ^{1}H NMR spectra. NOE correlations were observed between hydroquinol or naphthoquinol, and adjacent methylene protons of the strap and phenylene, bipyridinium and methylene protons of the macrocycle.

Table 3. Selected proton chemical shift values (δ, ppm) for the naphthoquinol-containing strapped porphyrin [2]catenanes **14**, **15**, and **16** under conditions of fast and slow exchange

[a]	**16** (slow)[b]	**15** (slow)	**15** (fast)[c]	**14** (fast)[d]
α	"outside" 8.52	"outside" 9.1	8.28	8.35
	"inside" 7.40	"inside" 8.22		
	"outside" 8.50	"outside" 8.78		
	"inside" 6.83	"inside" 8.11		
β	"outside" 6.99	"outside" 7.59	6.66	6.59
	"inside" 3.28	"inside" 4.21[e]		
	"outside" 7.13	"outside" 7.40		
	"inside" 3.39	"inside" 3.04[e]		
$-C_6H_4-$	7.80	7.89	7.43	7.63
	7.67	7.66		
$^+NCH_2$	5.60	5.83	5.29	5.32
	5.12	5.68		
	5.02	5.45		
NQ(α)	5.60[f]	5.83[f]	5.70	–
NQ(β)	5.30	5.66	5.18	–
NQ(γ)	1.47	1.75[f]	1.84	–

[a] Spectra were recorded at 300 MHz using the appropriate residual solvent as reference. [b] The [2]catenane **15** decomposed at temperatures above 380 K in [D_6]DMSO before the fast exchange limit could be attained. [c] Spectrum recorded in $(CD_3)_2SO$ at 360 K. [d] Spectrum recorded in $(CD_3)_2CO$ at 298 K; the slow exchange limit could not be reached at temperatures below −80 °C for **14**. [e] Hidden protons identified by saturation transfer techniques. [f] These proton resonances were hidden under larger peaks, but were identified from gradient NOE experiments.

From dynamic NMR measurements, it was possible to calculate rates for various processes observed in these catenanes, as we have established for the previous members of the series (Table 4). For the hydroquinol catenane **14**, a rotation rate of the macrocycle around the central hydroquinol of the strap (equivalent to an "inside" to "outside" exchange process for the bipyridinium rings on each side of the macrocycle) was calculated as 3.4×10^5 times per second at 25 °C. This relatively high value for the rotation of the tetracation is significantly greater than either **1c**: (n = 1, Ar = phenyl, M = Zn) (50 s^{-1} at 25 °C) or **1c**: (n = 2, Ar = phenyl, M = Zn) (2.5×10^3 s^{-1} at 25 °C) and implies that the major influence on the observed rotation rate of the tetracationic macrocycle in this series of porphyrin catenanes are steric factors. As this series demonstrates (Table 4), the short hydroquinol ether strap porphyrin catenane has a significant steric barrier to tetracation rotation, whereas the longer strapped derivatives are not as sterically restricted allowing free rotation of the macrocycle, particularly in **14**, which shows much less inhibited dynamic behaviour than the simpler, nonporphyrinic analogous catenanes **2a** of the Stoddart type.

In the case of the naphthoquinol porphyrin catenanes, a second exchange process was observed. In the case of the longer strapped naphthoquinol analogue **15**, tetracation resonances were broad at 30 °C, and only at 360 K in [D_6]DMSO were sharp resonances for all protons observed. At −80 °C in [D_6]acetone, eight bipyridinium peaks and two phenylene ($-C_6H_4-$) peaks as well as multiplets for the $^+NCH_2$ resonances were observed for the tetracation macrocycle. As was observed in the triethylene-strapped analogue **1c**: (n = 2, Ar = naphthyl, M = Zn), at −80 °C the ethyl and methyl groups of the porphyrin periphery are split into two methyl singlets and two ethyl multiplets, with the diastereotopic methylene resonances remaining as multiplets. These results can be rationalised in terms of two processes. The first is the slowing of the tetracation rotation about the naphthoquinol axis to distinguish between "inside" and "outside" tetracation environments, as for the hydroquinol porphyrin catenane. This rotation rate of the tetracation macrocycle was found to be 1.0×10^2 times per second at 25 °C.

The second effect that results in the additional splitting that is observed in the tetracation resonances in **15** over that observed for **14** has been interpreted in both porphyrin and nonporphyrinic catenanes as a local twofold symmetry of the naphthalene ring affecting both the tetracation and porphyrin moieties in the catenane. In **15**, the effects of this

Table 4. Kinetic and thermodynamic parameters from the dynamic ^1H NMR studies on the porphyrin [2]catenanes for tetracation rotation and reorientation

Catenane	Δν (Hz)	T_c (°C)	k_c (s^{-1})	$\Delta G_c^{\ddagger}$ (kJ·mol^{-1})	Rates at 25 °C (Hz)[a]
Rotation[a]					
2a					2000[a]
1c: n = 1, Ar = φ					50[a]
1c: n = 2, Ar = φ					2500[a]
1c: n = 3, Ar = φ (**14**)	62	−80	138	39	340 000[a]
2b					1200[a]
1c: n = 1, Ar = naphthyl (**16**)					0[a]
1c: n = 2, Ar = naphthyl					10[a]
1c: n = 3, Ar = naphthyl (**15**)	57	+19	127	60	100[a]
Reorientation[b]					
2b					10[b]
1c: n = 1, Ar = naphthyl (**16**)	18	+58	40	71	2[b]
1c: n = 2, Ar = naphthyl					400[b]
1c: n = 3, Ar = naphthyl (**15**)	79	−55	175	43	110 000[b]

[a] Data obtained by the coalescence method as previously reported. [b] Refers to the "out, turn around, and in again" process observed in naphthoquinol catenanes.

symmetry disappear from the spectrum at −55 °C as the two methyl singlet resonances coalesce, which has been explained before as a process involving the decomplexation of the naphthalene ring from within the tetracation macrocycle, a reorientation of the ring, followed by recomplexation. This phenomenon, dubbed the "out, turn around, and in again" process was measured using the coalescence method by following the methyl resonances, and was found (Table 4) to have a rate at 25 °C of 1.1×10^5 times per second.

In contrast to **15**, the tight strapped analogue **16** was found to have eight bipyridinium resonances, two phenylene singlets and $^{+}NCH_2$ peaks at 30 °C (as opposed to −80 °C for **15**), which indicates that this catenane undergoes slow exchange on the NMR time scale at this temperature, and not unexpectedly, reflects the severe steric restriction imposed by the short-strapped porphyrin on tetracation rotation. Hence, the rotation rate of the tetracation subunit in this catenane could not be measured since the "inside" and "outside" bipyridinium environments failed to coalesce before decomposition started to set in above 380 K in [D_6]DMSO. Nevertheless, the naphthalene "out, turn around, and in again" exchange process could still be measured at lower temperatures by following the coalescence of the two "outside" β-bipyridinium resonances. This process was found to be about 2 rotations per second at ambient temperatures and can be compared to the other naphthoquinol porphyrin catenanes, where the rates for this process increase from 4.0×10^2 s^{-1} to 1.1×10^5 s^{-1} at 25 °C as the length of the strap increases from triethylene to the tetraethylene glycol derivatives. This reflects the stronger π−π interaction of the naphthoquinol ring within the tetracation in the tighter-strapped porphyrin catenane.

In comparison to the hydroquinol porphyrin catenane **14**, the tetracation rotation rate (3.4×10^5 s^{-1} at 25 °C), the naphthoquinol porphyrin catenane **15** rotation rate is significantly slower. This is hardly surprising considering the relative sizes of the π-clouds and thus the expected stronger π−π interactions between the naphthoquinol ring and the tetracations.

An interesting comparison can also be made between the naphthoquinol porphyrin catenane **15** and its nonporphyrinic counterpart, namely, the 1,5-DN38C10-based [2]catenane **2b**. The observed tetracation rotation rate in the latter was found to be 1200 times per second at ambient temperature with a $\Delta G_c^{\ddagger}$ of 53.1 kJ·mol^{-1}, whereas the "out, turn around, and in again" process occurred at a rate of 10 times per second at 25 °C. By comparison, the porphyrin catenane analogue **15** (Table 4) has a substantially increased rate of removal-reorientation-recomplexation for the naphthoquinol ring (about four orders of magnitude) due to a lower activation energy, yet has a slower tetracation rotation rate (about one order of magnitude) resulting from a higher free energy of activation. This implies that the presence of the porphyrin subunit leads to a higher activation energy for tetracation rotation due to either a steric or electronic influence. However, the origin of the lower activation energy for the naphthoquinol decomplexation is not as evident, but it has been suggested that this may be as a result of the porphyrin catenane being conformationally less flexible than its nonporphyrinic counterpart, and that the number of sites available for [CH···O] hydrogen bonding (which as has been identified as an important stabilising force in noncovalent interactions) has been halved.[8]

UV/Vis Spectra

The absorption data for the catenanes are collected in Table 5 together with the data of the related porphyrin models **1a**, and the complexes with paraquat **1b**.[6,12] It is interesting to note that the ground state spectrum of **10b** shows few if any anomalous features, although the solid-state structure clearly identifies a planar distortion in the form of a ruffling of the porphyrin nucleus undoubtedly as a result of the "tight" strap; the less constrained **7b** shows no significant related distortion. The origins of a red shift in the absorption spectra of both B and Q bands as either a cause or effect relationship of distortions of the porphyrin nucleus from planarity, either in a ruffling or saddling mode, have been argued for several years, until very recently Ghosh and co-workers[25] have shown that such a correlation is not definitive, especially for free base or zinc (amongst others) derivatives. Nevertheless, even previous calculations by DiMagno et al[26] have implied that spectral red-shifts are a result of distortions allowing some rotation

Table 5. UV/Vis absorption properties of the porphyrins, the complexes and the catenanes at 298 K in acetonitrile solution. The charge-transfer bands (CT) arise from the interaction of the porphyrin with the paraquat or cyclobis-paraquat unit

	Soret bands λ_{max}/nm ($10^{-3}\varepsilon$/ M^{-1}cm^{-1})	Q bands λ_{max}/nm ($10^{-3}\varepsilon$/ M^{-1}cm^{-1})	Q bands λ_{max}/nm ($10^{-3}\varepsilon$/ M^{-1}cm^{-1})	CT bands
10b	414 (420)	542 (17.6)	577 (6.0)	
7b	413 (420)	542 (19.0)	577 (6.0)	
9b	413 (370)	542 (17.3)	577 (5.7)	
10b − PQ^{2+}	420 (224)	546 (15.0)	578 (5.1)	720 (260)
7b − PQ^{2+}	418 (257)	544 (17.0)	578 (6.7)	720 (230)
9b − PQ^{2+}	418 (234)	543 (15.0)	578 (5.8)	720 (380)
16	425 (199)	548 (21.1)	582 (7.4)	765 (600)
14	425 (210)	548 (18.8)	583 (5.8)	760 (400)
15	425 (201)	548 (21.7)	582 (6.9)	760 (500)

of the meso aryl groups from a perpendicular orientation with respect to the porphyrin plane to allow some degree of π-overlap with the porphyrin system. Clearly in the case of **10b**, the strap coming from both *o*-positions of the aryl groups will effectively prevent any such rotation, even in a distorted structure (and it is not unreasonable to assume that the solution structure of **10b** would show similar distortion, given the restrictions of the diethylene glycol strap). Thus the absence of a red shift is consistent with explanations advanced by both Ghosh and DiMagno, and explains the similarity in absorption spectra for all the derivatives described here.

The catenane spectra display typical porphyrin Soret and Q bands but they appear broader, shifted to lower energies and with lower molar absorption coefficients than the parent porphyrins and, to some extent, also with respect to the complexes **1b**.[6] In addition, for the catenanes new spectral features appear at lower energies than the Q-bands. These, displaying maxima around 760 nm and extinction coefficients in the range 10^2-10^3 $M^{-1}\cdot cm^{-1}$, are assigned to CT bands originated from the interaction between the porphyrin component and the paraquat units of the macrocycle in the catenanes. Similar bands, though less intense and with maxima at higher energies, were also observed for the complexes.[11] A stronger interaction is detected in the catenanes with respect to the complexes as revealed by the higher stabilization in the energy of the CT bands (lower wavelength), and higher absorption coefficients. The reason for such better stabilization in catenanes could be the higher oxidizing ability of the tetracationic macrocycle cyclo-bisparaquat(4,4′-biphenylene) ($CBPQ^{4+}$) compared to paraquat (PQ^{2+}),[12] but to some extent geometric factors could also play a role. In fact the rigidity of the catenane can ensure a better parallel orientation of the electron acceptor with the porphyrin plane, compared to the looser complex. Other CT bands deriving from the interaction between the $CBPQ^{4+}$ and the dimethoxy-aromatic group in the 450−520 region, in agreement with previous observations,[27] are also detectable, but mostly obscured by the intense Soret bands. The above features in the absorption spectra are indicative of interactions between the various components. Nonetheless, the units maintain their own independent spectral features, indicating that the interaction between components can be considered weak, although active in promoting electronic coupling as evidenced by fluorescence and electrochemical studies.[6]

Conclusion

The successful synthesis of the porphyrin [2]catenanes described here completes a set of six structures where the length of the polyethylene glycol strap over the porphyrin is regularly increased from diethylene to triethylene to tetraethylene, and the central electron-donor component is either hydroquinol- or naphthoquinol-based.

A complication that has been encountered with the chosen "2+2" route to the porphyrins, by condensation of a dipyrromethane with a pre-formed dialdehyde strap, is the co-formation of "straight" and "twisted" atropisomers in the longer strapped derivatives, and dimeric and higher oligomeric structures for the shorter straps. Although the atropisomers for both the hydroquinol and naphthoquinol-strapped porphyrins with tetraethylene glycol-based straps can be separated and structurally identified, they can be equilibrated in solution, and catenation under high pressure conditions of either an equilibrated mixture or the individual isomers, results in only a single [2]catenane in each case.

For each of the untwisted singly-strapped porphyrins, there is significant binding of the paraquat within the cavity formed by the strap, and the binding constants range over about two orders of magnitude. Nevertheless, the template-directed self-assembly process operates successfully in all cases, and good to moderate yields of catenanes are obtained under high pressure conditions.

For the catenanes, in each case the overall structural motif is the same, with the bipyridinium side of the macrocyclic ring oriented parallel to the porphyrin plane, so that the bipyridinium rings, the quinol, and the porphyrin are stacked in a face-to-face fashion. This is similar to the structures observed for the simple complexes between the corresponding strapped porphyrins and paraquat.

The temperature-dependent dynamic properties of the catenanes described here indicate a trend within the rates of rotation of the macrocycle around the central quinol axis, which are critically dependent on the length of the strap on the one hand, and on the nature of the quinol unit on the other. Within the hydroquinol serries, the rates of rotation increase from 50 to 25 000 to 340 000 s^{-1} at room temperature as the length of the strap increases by one ethylene glycol unit on each side. This compares with a rate of about 2 000 for the related nonporphyrinic analogue from the simple BPP34-C-10 [2]catenane, and indicates that the relatively large π-surface of the porphyrin provides an effective ′brake′ on the macrocycle rotation in the tight-strapped derivatives, but has little influence when the strap is loose enough not to impose any steric restriction.

For the similarly sized naphthoquinol derivatives, which have an increased π-surface area, the rotation rates are reduced by many orders of magnitude, ranging from essentially zero to 10 to 100 times per second at 25 °C through the same increase in chain length as for the hydroquinol analogues. This compares to the modest decrease in rate for the simple nonporphyrinic 1,5-DN38-C-10 [2]catenane compared to its phenyl analogue (1 200 vs. 2 000). It is thus apparent that π-π interactions between the naphthoquinol and porphyrin are sufficiently strong to cause a significant barrier to rotation. Nevertheless, a second process needs to be considered in the naphthoquinol cases − that of a barrier imposed by a process described as "out, turn around and in again", as a mechanism by which the naphthoquinol unit can rotate only by slipping out from the enclosing macrocycle first. This ranges from 2 to 400 to 110 000 s^{-1} at 25 °C in this porphyrin series, compared to about 10 for the nonporphyrinic analogue. Clearly, this is not a significant barrier to rotation in the porphyrin catenanes, and may

arise from the porphyrin catenane being conformationally less flexible than its nonporphyrinic counterpart, and having fewer sites available for [CH···O] hydrogen bonding.

A stronger π-π interaction as a the major influence in restricting rotation in the naphthoquinol series compared to the hydroquinol series, is indicated by the stronger binding constants of the corresponding strapped porphyrins for the simple guest paraquat. However, the electronic spectra of the catenanes themselves do not show any significantly enhanced charge-transfer bands over the hydroquinol counterparts.

With this set of catenanes in hand, we are now in a position to delineate their structure-activity profile by studying their behaviour under a range of stimuli, including chemical (acid/base), redox, and photochemical studies. This has been commenced with certain members of the series,[6,9,12] but we are now in a position to provide a complete catalogue of their fundamental properties, to allow a more systematic and rational structure-activity relationship across the whole series.

Experimental Section

General Remarks: All solvents were distilled before use, using standard procedures: tetrahydrofuran (THF) was distilled from over benzophenone and sodium under N_2; triethylamine (Et_3N) was distilled from over CaH_2; dimethylformamide (DMF) was dried with type 4Å molecular sieves. Column chromatography used Aldrich silica gel (grade 9385, 230−400 mesh). Preparative TLC was performed on 20 × 20 cm plates coated with 0.5 mm thick Art. 7731 Kieselgel 60 G Merck silica. Analytical TLC was carried out on Merck Silica Gel 60 G_{254} precoated aluminium sheets.

^{1}H NMR spectra were acquired using a 300 MHz Bruker Avance 300 spectrometer at 303 K, unless otherwise stated. Chemical shifts (δ) are reported in parts per million relative to residual solvent. Coupling constants (*J*) are reported in Hz. Deuterated solvents were purchased from Aldrich and stored over type 3Å molecular sieves after opening. COSY-45, gradient COSY, one-bond C−H correlation (HMQC), long-range C−H correlation (HMBC), NOESY, gradient NOESY two-dimensional NMR experiments employed the standard Bruker parameters. DEPT, NOE difference and saturation transfer experiments, as well selective gradient NOE experiments utilised standard Bruker pulse programs. UV/Vis spectra were recorded with a Varian Cary IE UV−VIS spectrophotometer. Melting points were determined using a Reichert microscopic hot-stage apparatus. FAB and ESI mass spectrometry was carried out by CSIRO Molecular Science at the Ian Wark Laboratory, Clayton and the Australian National University, Canberra, and high resolution ESI was performed at the Centre for Molecular Architecture, Rockhampton.

1,4-Bis[2-(2-{2-[2-(*o*-formylphenoxy)ethoxy]ethoxy}ethoxy)-ethoxy]benzene (4, *n* = 3): The hydroquinol bistosylate **3** (*n* = 3) (16.1 g, 2.08 × 10^{-2} mol) in dry CH_3CN (220 mL) was added all at once to a stirred mixture of salicylaldehyde (5.6 g, 4.58 × 10^{-2} mol) and K_2CO_3 (11.5 g, 8.32 × 10^{-2} mol) in dry CH_3CN (180 mL) with heating under an atmosphere of N_2 for 4 days. Upon cooling, the reaction mixture was filtered, the solid washed (CH_2Cl_2), the solvent removed by rotary evaporation, and the residue partitioned between CH_2Cl_2 and H_2O. The organic layer was separated, washed (H_2O), and dried ($MgSO_4$). The product was purified using column chromatography (silica) by eluting with CH_2Cl_2/petroleum ether (1:1), CH_2Cl_2/petroleum ether (2:1), and then CH_2Cl_2 to remove impurities, followed by MeOH/CH_2Cl_2 (1 %) to give **4** (*n* = 3) as a yellow oil (9.41 g, 67 %). $C_{36}H_{46}O_{12}$ (670.74): calcd. C 64.46, H 6.91; found C 64.20, H 6.84. ^{1}H NMR (300 MHz. $CDCl_3$, 25 °C): δ = 10.50 (d, *J* = 1 Hz, 2 H, CHO), 7.81 (dd, *J* = 8, 2 Hz, 2 H, Ar-H), 7.51 (dt, *J* = 8, 2 Hz, 2 H, Ar-H), 7.01 (t *J* = 8 Hz, 2 H,, Ar-H), 6.96 (d, *J* = 8Hz, 2 H, Ar-H), 6.80 (s, 4 H, Ar-H), 4.22 (t, 4 H, *J* = 5 Hz, OCH_2), 4.04 (t, *J* = 5 Hz, 4 H, OCH_2), 3.90 (t, *J* = 5 Hz, 4 H, OCH_2), 3.80 (t, *J* = 5 Hz, 4 H, OCH_2), 3.72−3.65 (m, 16 H, OCH_2) ppm.

Hydroquinol-Strapped Porphyrins 6 and 7: Hydroquinol dialdehyde **4:** *n* = 3 (2.55 g, 3.80 mmol) and 3,3′-diethyl-4,4′-dimethyl-2,2′-dipyrrylmethane (**5**) (1.75 g, 7.60 mmol) were dissolved with stirring in MeOH (380 mL), then bubbled with N_2 for 10 min, before adding a solution of Cs_2CO_3 (1.49 g, 4.56 mmol) and TFA (1.04 g, 9.12 mmol) in MeOH (15 mL). The reaction mixture was bubbled with N_2 for a further 5 min, before adding catalytic amounts of TFA (≈ 0.5 g), stirring for 5 h (room temp., N_2, dark), adding *o*-chloranil (1.87 g, 7.60 mmol) in THF (62 mL) all at once, and stirring continued overnight (room temp., dark). Then Et_3N (10 mL) was added, stirred for 30 min, and the solution taken to dryness by rotary evaporation. An initial purification was carried out on an alumina column using CH_2Cl_2 as the eluent to obtain several porphyrin fractions. A final purification was carried out by column chromatography (silica), eluting initially with C 2Cl_2 and CH_2Cl_2/Et_2O (5 %) to remove impurities followed by CH_2Cl_2/Et_2O (8 %) and then CH_2Cl_2/Et_2O (10 %) to obtain the porphyrin isomer **6a**, and then CH_2Cl_2/Et_2O (15 %) and CH_2Cl_2/Et_2O (20 %) to obtain **7a**.

6a was recrystallised to obtain a purple/red solid (101 mg, 2 %), m.p. 185−188 °C (from CH_2Cl_2/MeOH). $C_{66}H_{80}N_4O_{10}·H_2O$ (1107.38): calcd. C 71.58, H 7.46, N 5.06; found C 71.71, H 7.42, N 4.66. ESMS: *m*/*z* = $[M + H]^+$ 1089.6002 (calcd. 1089.5957), $[M + 2H]^{2+}$ 545.3011 (calcd. 545.3018). UV ($CHCl_3$): λ = 410, 508, 541, 575, 627 nm. ^{1}H NMR (300 MHz, $CDCl_3$, 25 °C): δ = 10.10 (s, 2 H, *meso*-H), 7.74 (t, *J* = 7 Hz, 2 H, Ar-H), 7.73 (d, *J* = 7 Hz, 2 H, Ar-H), 7.34 (d, *J* = 7 Hz, 2 H, Ar-H), 7.32 (t, *J* = 7 Hz, 2 H, Ar-H), 6.91 (s, 4 H, Ar-H), 4.14 (t, *J* = 5 Hz, 4 H, OCH_2), 3.98−3.88 (m, 12 H, CH_2CH_3 + OCH_2), 3.44 (t, *J* = 5 Hz, 4 H, OCH_2), 3.18 (t, *J* = 5 Hz, 4 H, OCH_2), 3.01 (t, *J* = 5 Hz, 4 H, OCH_2), 2.67 (t, *J* = 5 Hz, 4 H, OCH_2), 2.50 (s, 12 H, CH_3), 2.28 (t, *J* = 5 Hz, 4 H, OCH_2), 2.19 (m, 4 H, OCH_2), 1.69 (t, *J* = 8 Hz, 12 H, CH_2CH_3), 1.24 (s, 2 H, H_2O), −2.42 (br. s, 2 H, pyrrole NH) ppm. ^{13}C NMR ($CDCl_3$): δ = 158.52, 153.15, 145.28, 144.12, 140.79, 135.65, 134.54, 131.11, 129.942, 120.87, 115.93, 113.95, 111.79, 95.86, 70.64, 70.08, 69.89, 69.66, 69.47, 69.33, 68.79, 68.22, 19.82, 17.69, 13.64 ppm.

7a was recrystallised to obtain a purple/red solid (294 mg, 7 %), m.p. 166−169 °C (from CH_2Cl_2/MeOH). $C_{66}H_{80}N_4O_{10}·H_2O$ (1107.38): calcd. C 71.58, H 7.46, N 5.06; found C 71.74, H 7.34, N 5.00. ESMS: *m*/*z* = $[M + H]^+$ 1090.0 (calcd. 1089.6), $[M + 2H]^{2+}$ 545.6 (calcd. 545.3). UV ($CHCl_3$): λ = 410, 507, 541, 575, 626 nm. ^{1}H NMR (300 MHz. $CDCl_3$, 25 °C): δ = 10.17 (s, 2 H, *meso*-H), 7.74 (t, *J* = 7 Hz, 2 H, Ar-H), 7.65 (d, *J* = 7 Hz, 2 H, Ar-H), 7.33 (d, *J* = 9 Hz, 2 H, Ar-H), 7.31 (t, *J* = 7 Hz, 2 H, Ar-H), 6.13 (s, 4 H, Ar-H), 4.14 (t, *J* = 5 Hz, 4 H, OCH_2), 4.05−3.93 (m, 8 H, CH_2CH_3), 3.15 (m, 8 H, OCH_2), 2.80 (t, *J* = 4 Hz, 4 H, OCH_2), 2.64 (s, 8 H, OCH_2), 2.55 (s, 12 H, CH_3), 2.55−2.48 (m, 8 H, OCH_2), 1.78 (t, *J* = 8 Hz, 12 H, CH_2CH_3), 1.24 (s, 2 H, H_2O), −2.37 (br. s, 2 H, pyrrole NH) ppm.

Zinc Hydroquinol-Strapped Porphyrin 6b: Zinc was inserted into the hydroquinol porphyrin isomer **6a** to give **6b**, which was recrystallised to obtain a purple/pink solid, m.p. 198−200 °C (from CH_2Cl_2/MeOH). UV ($CHCl_3$): λ = 412, 504, 540, 574 nm. ^{1}H NMR (300 MHz. $CDCl_3$, 25 °C): δ = 10.06 (s, 2 H, CHO), 7.71 (t, *J* = 8 Hz, 2 H, Ar-H), 7.61 (d, *J* = 9 Hz, 2 H, Ar-H), 7.38 (d, *J* = 8 Hz, 2 H, Ar-H), 7.26 (t, *J* = 8 Hz, 2 H, Ar-H), 6.72 (s, 4 H, Ar-H), 4.16 (t, *J* = 5 Hz, 4 H, OCH_2), 3.94 (q, *J* = 8 Hz, 8 H, CH_2CH_3), 3.53 (t, *J* = 5 Hz, 4 H, OCH_2), 3.24 (t, *J* = 5 Hz, 4 H, OCH_2), 3.03 (t, *J* = 5 Hz, 4 H, OCH_2), 2.62 (t, *J* = 5 Hz, 4 H, OCH_2), 2.48 (s, 12 H, CH_3), 2.42 (m, 8 H, OCH_2), 2.29 (t, *J* = 5 Hz, 4 H, OCH_2), 1.70 (t, *J* = 8 Hz, 12 H, CH_2CH_3) ppm.

Zinc Hydroquinol-Strapped Porphyrin 7b: Zinc was inserted into the hydroquinol (4)-porphyrin H_2HQ4P (**17a**) to give (**17b**), which was recrystallised to obtain a purple/pink solid, m.p. 166−168 °C (from CH_2Cl_2/MeOH). UV ($CHCl_3$ (1 %)/MeCN): λ (ε, $M^{-1}cm^{-1}$) = 413 (4.26×10^5), 504 (3.64×10^3), 542 (1.94×10^4), 576 (7.58×10^3) nm. ^{1}H NMR (300 MHz, $CDCl_3$, 25 °C): δ = 10.09 (s, 2 H, CHO), 7.74 (t, *J* = 8 Hz, 2 H, Ar-H), 7.71 (d, *J* = 7 Hz, 2 H, Ar-H), 7.32 (t, *J* = 7 Hz, 2 H, Ar-H), 7.31 (d, *J* = 8 Hz, 2 H, Ar-H), 6.12 (s, 4 H, Ar-H), 4.10 (t, *J* = 5 Hz, 4 H, OCH_2), 3.99 (m, 8 H, CH_2CH_3), 3.09 (t, *J* = 5 Hz, 4 H, OCH_2), 2.84 (t, *J* = 4 Hz, 4 H, OCH_2), 2.52 (s, 12 H, CH_3), 2.46 (t, *J* = 5 Hz, 4 H, OCH_2), 2.34 (m, 8 H, OCH_2), 2.12 (s, 8 H, OCH_2), 1.76 (t, *J* = 7 Hz, 12 H, CH_3CH_2) ppm.

Zinc Hydroquinol-Strapped Porphyrin [2]Catenane 14b: A mixture of the hydroquinol-strapped porphyrin isomers **6a** and **7a** were refluxed in MeCN for 1 h to reach equilibrium, before zinc was inserted to produce a mixture of **6b** and **7b**. The mixed isomers [**6b** (12 %) and **7b** (88 %), from ^{1}H NMR] (130 mg, 1.13×10^{-4} mol), 1,1′-[1,4-phenylenebis(methylene)]-bis(4,4′-bipyridinium) bis(hexafluorophosphate) (**13**)[28] (96 mg, 1.36×10^{-4} mol), 1,4-bis(bromomethyl)benzene (45 mg, 1.70×10^{-4} mol), and catalytic amounts of NaI and NH_4PF_6 were dissolved in DMF (7 mL), deoxygenated with N_2 for 20 min, and then stirred at room temperature at 12 kbar for 3 days. The solvent was then removed under vacuum with heating, and the residue was washed well with CH_2Cl_2, followed by hot H_2O. Purification was carried out by column chromatography (silica) by eluting initially with CH_2Cl_2/MeOH (10 %), followed by MeOH/2 M NH_4Cl solution/$MeNO_2$ (7:2:1, v/v). The product fractions were taken to dryness, the residue dissolved in a minimum amount of MeOH/H_2O and acetone, and a solution of $Zn(OAc)_2$ in MeOH was added and allowed to stir at room temperature for one hour. The solvent was then removed, the residue dissolved in MeOH, and the product precipitated with H_2O. The material was then filtered, the solid dissolved in a minimum amount of MeOH, and saturated NH_4PF_6 solution added until no further precipitation was evident. The catenane product was collected by filtration, washed (H_2O), and pumped dry. The product was recrystallised to obtain **14b** as a dark purple solid (33 mg, 13 %), m.p. 230−234 °C (from acetone/*i*Pr_2O). $C_{102}H_{110}N_8O_{10}P_4F_{24}Zn$ (2253.26): calcd. C 54.37, H 4.92, N 4.97; found C 54.01, H 5.26, N 4.66. FAB MS: *m*/*z* = $[M - PF_6^-]^+$ 2106.3 (calcd. 2105.7), $[M - 2PF_6^-]^+$ 1961.3 (calcd. 1960.7), $[M - 3PF_6^-]^+$ 1816.4 (calcd. 1815.7), $[M - 4PF_6^-]^+$, [M − tetracation − $4PF_6^-]^+$ 1149.9 (calcd. 1150.5). UV (acetone): λ = 408, 506, 540, 574 nm. ^{1}H NMR (300 MHz, [D_6]acetone, 25 °C): δ = 9.99 (s, 2 H, *meso*-H), 8.28 (d, *J* = 7 Hz, 8 H, α-bipy), 7.86 (dt, *J* = 8 Hz, 2 Hz, 2 H, Ar-H), 7.63 (d, *J* = 8 Hz, 2 H, Ar-H), 7.43 (s, 8 H, $-C_6H_4-$), 7.42 (d, *J* = 8 Hz, 2 H, Ar-H), 7.36 (t, *J* = 7 Hz, 2 H, Ar-H), 6.66 (d, *J* = 7 Hz, 8 H, β-bipy), 5.29 (s, 8 H, $^+N-CH_2$), 4.53 (br. s, 4 H, OCH_2), 4.17 (m, 4 H, CH_2CH_3), 3.87 (m, 4 H, CH_2CH_3), 3.83 (br. s, 4 H, OCH_2), 3.75 (br. s, 4 H, OCH_2), 3.66 (br. s, 8 H, OCH_2), 3.55 (br. s, 8 H, OCH_2), 3.15 (br. s, 4 H, OCH_2), 3.00 (s, 4 H, Ar-H), 2.62 (s, 12 H, CH_3), 1.73 (t, 12 H, *J* = 7 Hz, CH_2CH_3) ppm.

1,5-Bis[2-(2-{2-[2-(*o*-formylphenoxy)ethoxy]ethoxy}ethoxy)-ethoxy]naphthalene (4, *n* = 3, Ar = naphthyl): Salicylaldehyde (1.27 g, 10.4 mmol) and K_2CO_3 (2.61 g, 18.9 mmol) were stirred in dry CH_3CN (40 mL) with heating under N_2 for 1 h. Then naphthoquinol bistosylate **3** (*n* = 3, Ar = naphthyl) (4.01 g, 6.22 mmol) in dry CH_3CN (120 mL) was added all at once, and the resulting solution refluxed under N_2 for 3 days. Upon cooling, the solvent was removed by rotary evaporation, and the residue partitioned between CH_2Cl_2 and H_2O. The organic layer was separated, washed (H_2O), and dried ($MgSO_4$). The product was purified using column chromatography (silica) by eluting with C $_2Cl_2$ to remove impurities, followed by MeOH/CH_2Cl_2 (1 %) to give **4** (*n* = 3, Ar = naphthyl) as a yellow oil (2.37 g, 70 %); found C 66.48, H 7.01. $C_{40}H_{48}O_{12}$ (720.80) requires C, 66.65, H 6.71 %. ^{1}H NMR (300 MHz. $CDCl_3$, 25 °C): δ = 10.49 (s, 2 H, CHO), 7.84 (d, *J* = 8 Hz, 2 H, Ar-H), 7.80 (dd, *J* = 8, 2 Hz, 2 H, Ar-H), 7.49 (dt, *J* = 7, 2 Hz, 2 H, Ar-H), 7.31 (t, *J* = 8 Hz, 2 H, Ar-H), 6.70 (t, *J* = 8 Hz, 2 H, Ar-H), 6.91 (d, *J* = 8 Hz, 2 H, Ar-H), 6.80 (d, *J* = 8 Hz, 2 H, Ar-H), 4.26 (t, *J* = 5 Hz, 4 H, OCH_2), 4.17 (t, *J* = 5 Hz, 4 H, OCH_2), 3.97 (t, *J* = 5 Hz, 4 H, OCH_2), 3.86 (t, *J* = 5 Hz, 4 H, OCH_2), 3.79 (m, 4 H, OCH_2), 3.69 (m, 12 H, OCH_2) ppm.

Naphthoquinol-Strapped Porphyrins 8 and 9: Naphthoquinol dicarbaldehyde **4** (*n* = 3, Ar = naphthyl) (0.97 g, 1.35 mmol) and 3,3′-diethyl-4,4′-dimethyl-2,2′-dipyrrylmethane (**5**) (0.62 g, 2.7 mmol) were dissolved with stirring in MeOH (135 mL), bubbled with N_2 for 10 min, and then catalytic amounts of TFA (≈ 10 drops) were added. The reaction mixture was then stirred for 5 h (room temp., N_2, dark), before adding *o*-chloranil (0.66 g, 2.7 mmol) in THF (21 mL) all at once and stirring was continued overnight (room temp., dark). Then was added Et_3N (4 mL) and the mixture stirred for 30 min, before taking the solution to dryness by rotary evaporation. An initial purification was carried out on an alumina column using CH_2Cl_2 and then CH_2Cl_2/Et_2O (10 %) to remove impurities, followed by CH_2Cl_2/Et_2O (15 %) to elute several porphyrin fractions. A final purification was carried out by column chromatography (silica), eluting initially with C $_2Cl_2$ and CH_2Cl_2/Et_2O (5 %) followed by CH_2Cl_2/Et_2O (10 %) to obtain the porphyrin isomer **8a**, and then CH_2Cl_2/Et_2O (15 %) to obtain **9a**.

8a was recrystallised to obtain a purple/red solid (99 mg, 6 %), m.p. 186−189 °C (from CH_2Cl_2/MeOH). $C_{70}H_{82}O_{10}N_4 \cdot 2H_2O$ (1175.45): calcd. C 71.52, H 7.38, N 4.77; found C 71.05, H 7.07, N 4.68. ESMS: *m*/*z* = $[M + H]^+$ 1140.0 (calcd. 1139.6). UV ($CHCl_3$): λ = 410, 507, 541, 575, 626 nm. ^{1}H NMR (300 MHz, $CDCl_3$, 25 °C): δ = 10.02 (s, 2 H, *meso*-H), 7.95 (d, *J* = 8 Hz, 2 H, Ar-H), 7.71 (dt, *J* = 8, 2 Hz, 2 H, Ar-H), 7.69 (d, *J* = 7 Hz, 2 H, Ar-H), 7.41 (t, *J* = 8 Hz, 2 H, Ar-H), 7.31 (d *J* = 8 Hz, 2 H, Ar-H), 7.26 (t, *J* = 7 Hz, 2 H, Ar-H), 6.86 (d, *J* = 8 Hz, 2 H, Ar-H), 4.23 (t, *J* = 4 Hz, 4 H, OCH_2), 4.11 (t, *J* = 4 Hz, 4 H, OCH_2), 3.80 (q, *J* = 7 H, 8 Hz, CH_2CH_3), 3.70 (t, *J* = 4 Hz, 4 H, OCH_2), 3.20−3.13 (m, 8 H, OCH_2), 2.75 (t, *J* = 5 Hz, 4 H, OCH_2), 2.42 (s, 12 H, CH_3), 2.25 (m, 4 H, OCH_2), 2.16 (m, 4 H, OCH_2), 1.58 (t, *J* = 7 Hz, 12 H, CH_2CH_3), 1.52 (s, 4 H, 2 H_2O), −2.47 (br. s, 2 H, pyrrole NH) ppm.

9a was recrystallised to obtain a purple/red solid (207 mg, 14 %), m.p. 178−180 °C (from CH_2Cl_2/MeOH). $C_{70}H_{82}N_4O_{10} \cdot 2H_2O$ (1175.45): calcd. C 71.52, H 7.38, N 4.77; found C 71.63, H 7.02, N 4.58. ESMS: *m*/*z* = $[M + H]^+$ 1140.1 (calcd. 1139.6), $[M + 2H]^{2+}$ 570.7 (calcd. 570.3). UV ($CHCl_3$): λ = 410, 507, 541, 574,

626 nm. ^{1}H NMR (300 MHz, $CDCl_3$, 25 °C): δ = 10.18 (s, 2 H, *meso*-H), 7.73 (dt, *J* = 7, 2 Hz, 2 H, Ar-H), 7.61 (dd, *J* = 7, 2 Hz, 2 H, Ar-H), 7.37 (d, *J* = 8 Hz, 2 H, Ar-H), 7.31 (d, *J* = 8 Hz, 2 H, Ar-H), 7.30 (t, *J* = 8 Hz, 2 H, Ar-H), 6.74 (t, *J* = 8 H, 2 Hz, Ar-H), 5.88 (d, *J* = 8 Hz, 2 H, Ar-H), 4.08 (t, *J* = 5 Hz, 4 H, OCH_2), 4.00 (q, *J* = 7 Hz, 8 H, CH_2CH_3), 3.23 (t, *J* = 4 Hz, 4 H, OCH_2), 3.05 (t, *J* = 5 Hz, 4 H, OCH_2), 2.91 (t, *J* = 4 Hz, 4 H, OCH_2), 2.70 (s, 8 H, OCH_2), 2.56 (s, 12 H, CH_3), 2.54 (m, 4 H, OCH_2), 2.47 (m, 4 H, OCH_2), 1.78 (t, *J* = 7 Hz, 12 H, CH_2CH_3), 1.52 (s, 4 H, $2H_2O$), −2.33 (br. s, 2 H, pyrrole NH) ppm.

Zinc Naphthoquinol-Strapped Porphyrin 8b: Zinc was inserted into the free base **8a** to give **8b**, which was recrystallised to obtain a purple/pink solid, m.p. 251−252 °C (from CH_2Cl_2/MeOH). $C_{70}H_{80}O_{10}N_4Zn{\cdot}2H_2O$ (1238.83): calcd. C 67.86, H 6.84, N 4.52; found C 68.18, H 6.68, N 4.22. UV ($CHCl_3$): λ = 415, 542, 577 nm. ^{1}H NMR (300 MHz, $CDCl_3$, 25 °C): δ = 10.02 (s, 2 H, *meso*-H), 7.80 (d, *J* = 8 Hz, 2 H, Ar-H), 7.70 (t, *J* = 8 Hz, 2 H, Ar-H), 7.58 (d, *J* = 8 Hz, 2 H, Ar-H), 7.38 (m, 4 H, Ar-H), 7.19 (t, *J* = 8 Hz, 2 H, Ar-H), 6.76 (d, *J* = 8 Hz, 2 H, Ar-H), 4.14 (m, 4 H, OCH_2), 3.92−3.82 [m, 12 H, CH_2CH_3 (8 H), OCH_2 (4 H)], 3.34 (t, *J* = 4 Hz, 4 H, OCH_2), 3.20 (m, 4 H, OCH_2), 2.82 (t, *J* = 4 Hz, 4 H, OCH_2), 2.54 (m, 4 H, OCH_2), 2.40 [s, 16 H, CH_3 (12 H), OCH_2 (4 H)], 2.32 (t, *J* = 3 Hz, 4 H, OCH_2), 1.65 (t, *J* = 8 Hz, 12 H, CH_2CH_3), 1.28 (s, 4 H, 2 H_2O) ppm.

Zinc Naphthoquinol-Strapped Porphyrin 9b: Zinc was inserted into **9a** to give **9b**, which was recrystallised to obtain a purple/pink solid, m.p. 109−111 °C (from CH_2Cl_2/MeOH). $C_{70}H_{80}O_{10}N_4Zn{\cdot}2H_2O$ (1238.83): calcd. C 67.86, H 6.84, N 4.52; found C 67.50, H 6.77, N 4.41. UV ($CHCl_3$): λ = 415, 542, 576 nm. ^{1}H NMR (300 MHz, $CDCl_3$, 25 °C): δ = 10.15 (s, 2 H, *meso*-H), 7.77 (d, *J* = 6 Hz, 2 H, Ar-H), 7.76 (t, *J* = 8 Hz, 2 H, Ar-H), 7.38−7.28 (m, 6 H, Ar-H), 6.93 (t, *J* = 8 Hz, 2 H, Ar-H), 6.07 (d, *J* = 7 Hz, 2 H, Ar-H), 4.07−3.98 [m, 12 H, CH_2CH_3 (8 H), OCH_2 (4 H)], 2.94 (t, *J* = 4 Hz, 4 H, OCH_2), 2.88 (t, *J* = 6 Hz, 4 H, OCH_2), 2.56 (s, 12 H, CH_3), 2.31 (s, 12 H, OCH_2), 2.02 (s, 8 H, OCH_2), 1.80 (t, *J* = 8 Hz, 12 H, CH_2CH_3), 1.28 (s, 4 H, 2 H_2O) ppm.

Naphthoquinol-Strapped Porphyrin [2]Catenane 15: A mixture of the naphthoquinol-strapped porphyrin isomers **8a** and **9a** were refluxed in MeCN and $CHCl_3$ for 3 h to obtain an equilibrium mixture, before zinc was inserted to produce a mixture of **8b** and **9b** (8 % and 92 %, respectively, from ^{1}H NMR integrations) (146 mg, 1.21×10^{-4} mol), 1,1′-[1,4-phenylenebis(methylene)]-bis(4,4′-bipyridinium) bis(hexafluorophosphate) **13**[28] (107 mg, 1.52×10^{-4} mol), 1,4-bis(bromomethyl)benzene (50 mg, 1.91×10^{-4} mol), and catalytic amounts of NaI and NH_4PF_6 were dissolved in DMF (7 mL), deoxygenated with N_2 for 20 min, and then stirred at room temperature at 12 KBar for 4 days. The solvent was then removed under vacuum with heating, and the residue was washed well with CH_2Cl_2, followed by hot H_2O. Purification was carried out by column chromatography (silica) by eluting initially with CH_2Cl_2/MeOH (10 %), followed by MeOH/2 M NH_4Cl solution/$MeNO_2$ (7:2:1, v/v). The product fractions were taken to dryness, the residue dissolved in a minimum amount of MeOH/H_2O and acetone, and a solution of $Zn(OAc)_2$ in MeOH was added and the mixture allowed to stir at room temperature for one hour. The acetone was then removed, the solution filtered, the solid dissolved in a minimum amount of MeOH/H_2O, and saturated NH_4PF_6 solution added until no further precipitation was evident. The catenane product was collected by filtration, washed (H_2O), and pumped dry. The product was then recrystallised to obtain catenane 15 as a dark purple solid (97 mg, 35 %), m.p. 221−224 °C (from acetone/iPr_2O). $C_{106}H_{112}O_{10}N_8P_4F_{24}Zn{\cdot}2H_2O$ (2339.35): calcd. C 54.33, H 4.99, N 4.78; found C 54.06, H 4.96, N 4.84. ESMS: *m*/*z* = $[M + H - PF_6]^+$ 2156.3 (calcd. 2156.7), $[M + H - \text{tetracation} - 4PF_6]^+$ 1201.4 (calcd. 1201.5), $[M + 2H - 2PF_6]^{2+}$ 1006.6 (calcd. 1006.4), $[M - 3PF_6]^{3+}$ 622.3 (calcd. 621.9), $[M - \text{tetracation} - 4PF_6]^{2+}$ 600.1 (calcd. 600.3), $[M + 4H]^{4+}$ 576 (calcd. 576.2), $[M + 4H - Zn]^{4+}$ 560.2 (calcd. 560.2), $[M - 4PF_6]^{4+}$ 430.1 (calcd. 430.2). UV (acetone): λ = 418, 545, 576 nm. ^{1}H NMR (300 MHz, [D_6]DMSO, 360 K): δ = 9.89 (s, 2 H, *meso*-H), 8.35 (d, *J* = 6 Hz, 8 H, α-bipy), 7.82 (t, *J* = 7 Hz, 2 H, Ar-H), 7.63 (s, 8 H, $-CH_4-$), 7.51 (d, *J* = 7 Hz, 2 H, Ar-H), 7.49 (dd, *J* = 7, 2 Hz, 2 H, Ar-H), 7.36 (t, *J* = 7 Hz, 2 H, Ar-H), 6.59 (d, *J* = 6 Hz, 8 H, β-bipy), 5.65 (d, *J* = 8 Hz, 2 H, Ar-H), 5.32 (s, 8 H, $^+N-CH_2$), 5.18 (t, *J* = 8 Hz, 2 H, Ar-H), 4.12 (t, *J* = 5 Hz, 4 H, OCH_2), 2.46 (s, 12 H, CH_3), 1.91 (s, 4 H, $2H_2O$), 1.84 (d, *J* = 8 Hz, 2 H, Ar-H), 1.70 (t, *J* = 7 Hz, 12 H, CH_2CH_3) ppm.

1,5-Bis{2-[2-(*o*-formylphenoxy)ethoxy]ethoxy}naphthalene (4, *n* = 1, Ar = naphthyl): Salicylaldehyde (1.67 g, 13.7 mmol) and K_2CO_3 (3.44 g, 24.9 mmol) were stirred in dry CH_3CN (55 mL) with heating under N_2 for 1 h. Then naphthoquinol bistosylate **3** (*n* = 1, Ar = naphthyl) (4.01 g, 6.22 mmol) in dry CH_3CN (190 mL) was added all at once, and the resulting solution refluxed under N_2 for 4 days. Upon cooling, the solvent was removed by rotary evaporation, and the residue partitioned between CH_2Cl_2 and H_2O. The organic layer was separated, washed (H_2O), and dried ($MgSO_4$). The product was purified using column chromatography (silica) by eluting with C $_2Cl_2$ and then CH_2Cl_2/petroleum ether (5 %) to remove impurities, followed by CH_2Cl_2/Et_2O (2 %) to give **4** (*n* = 1, Ar = naphthyl) as a yellow solid, which was recrystallised to yield a beige solid (2.69 g, 79 %), m.p. 121−123 °C (from $CHCl_3$/ethyl acetate). $C_{32}H_{32}O_8$ (544.59): calcd. C 70.58, H 5.92; found C 70.05, H 5.96. ^{1}H NMR (300 MHz, $CDCl_3$, 25 °C): δ = 10.53 (s, 2 H, CHO), 7.83 (dt, *J* = 7, 2 Hz, 4 H, Ar-H), 7.50 (dt, *J* = 8, 2 Hz, 2 H, Ar-H), 7.32 (t, *J* = 8 Hz, 2 H, Ar-H), 7.00 (dt, *J* = 8, 2 Hz, 2 H, Ar-H), 6.98 (d, *J* = 8 Hz, 2 H, Ar-H), 6.83 (d, *J* = 8 Hz, 2 H, Ar-H), 4.33−4.27 (m, 8 H, OCH_2), 4.08−4.04 (m, 8 H, OCH_2) ppm.

Naphthoquinol-Strapped Porphyrin 10b: Naphthoquinol dialdehyde **4** (*n* = 1, Ar = naphthyl) (0.5 g, 0.99 mmol) and 3,3′-diethyl-4,4′-dimethyl-2,2′-dipyrrylmethane (**5**) (0.45 g, 1.98 mmol) were dissolved with stirring in THF (100 mL). The solution was bubbled with N_2 for 20 min before adding catalytic amounts of *p*-toluenesulfonic acid. Stirring was continued for 48 h (room. temp., N_2, dark), and *o*-chloranil (485 mg, 1.97 mmol) in THF (10 mL) was added all at once, and stirring was further continued overnight (room. temp., dark). Then Et_3N (4 mL) was added, stirred for 45 min, and the solution taken to dryness by rotary evaporation. An initial purification was carried out on an alumina column using CH_2Cl_2 as the eluent, followed by a silica column using the same eluent. Zinc was then inserted into the porphyrin fractions, before a final purification was carried out on preparative TLC plates using CH_2Cl_2 as the eluent to obtain 3 different porphyrin fractions **10b**, **11b**, and a trimeric product.

10b was recrystallised to obtain a bright red solid (41.6 mg, 5 %), m.p. 318−322 °C, (from CH_2Cl_2/MeOH). $C_{62}H_{64}O_6N_4Zn{\cdot}2H_2O$ (1062.62): calcd. C 70.08, H 6.45, N 5.27; found C 70.12, H 6.51, N 5.05. ESMS *m*/*z* = $[M + H]^+$ 1025.8 (calcd. 1025.4). UV ($CHCl_3$ (1 %)/MeCN): λ = 414, 504, 542, 576 nm. ^{1}H NMR (300 MHz, $CDCl_3$, 25 °C): δ = 9.92 (s, 2 H, *meso*-H), 7.76 (dt, *J* = 8, 2 Hz, 2 H, Ar-H), 7.54 (dd, *J* = 8, 2 Hz, 2 H, Ar-H), 7.32−7.25 (m, 4 H, Ar-H), 5.55 (d, *J* = 8 Hz, 2 H, Ar-H), 4.65 (t, *J* = 8 Hz, 2 H, Ar-H), 4.30 (d, *J* = 8 Hz, 2 H, Ar-H), 4.26 (t, *J* = 4 Hz, 4 H, OCH_2), 3.94 (q, *J* = 7 Hz, 8 H, CH_2CH_3), 3.48 (t, *J* = 4 Hz, 4 H, OCH_2),

3.27 (t, J = 4 Hz, 4 H, OCH_2), 2.83 (t, J = 4 Hz, 4 H, OCH_2) 2.52 (s, 12 H, CH_3), 1.77 (t, J = 7 Hz, 12 H, CH_2CH_3), 1.50 (s, 4 H, $2H_2O$) ppm.

11b was recrystallised to obtain a red solid (9.6 mg, 1 %), m.p. 210−214 °C, (from CH_2Cl_2/MeOH). $C_{124}H_{128}O_{12}N_8Zn_2{\cdot}4H_2O$ (2125.23): calcd. C 70.08, H 6.45, N 5.27; found C 70.15, H 6.09, N 5.31. FAB MS: m/z = $[M + 4H]^+$ 2051.9 (calcd. 2052.85), $[M + 4H]^{2+}$ 1026.4 (calcd. 1026.43). UV ($CHCl_3$): λ = 412, 541, 576 nm. ^{1}H NMR (300 MHz, $CDCl_3$, 25 °C): δ = 10.20 (s, 2 H, *meso*-H), 9.80 (s, 2 H, *meso*-H), 7.75 (t, J = 6 Hz, 2 H, Ar-H), 7.72 (d, J = 6 Hz, 2 H, Ar-H), 7.66 (d, J = 7 Hz, 2 H, Ar-H), 7.60 (d, J = 6 Hz, 2 H, Ar-H), 7.38−7.25 (m, 8 H, Ar-H), 7.02 (d, J = 9 Hz, 2 H, Ar-H), 6.69 (d, J = 9 Hz, 2 H, Ar-H), 6.50 (t, J = 8 Hz, 2 H, Ar-H), 6.21 (t, J = 8 Hz, 2 H, Ar-H), 5.75 (d, J = 8 Hz, 2 H, Ar-H), 4.99 (d, J = 8 Hz, 2 H, Ar-H), 4.25 (t, J = 5 Hz, 4 H, OCH_2), 4.09 (t, J = 5 Hz, 4 H, OCH_2), 4.04 (m, 8 H, CH_2CH_3), 3.65 (m, 8 H, CH_2CH_3), 3.39 (t, J = 5 Hz, 4 H, OCH_2), 3.19 (t, J = 5 Hz, 4 H, OCH_2), 2.93 (t, J = 5 Hz, 4 H, OCH_2), 2.59 (s, 12 H, CH_3), 2.38 (s, 12 H, CH_3), 2.35 (t, J = 5 Hz, 4 H, OCH_2), 2.26 (t, J = 5 Hz, 4 H, OCH_2), 1.79 (t, J = 7 Hz, 12 H, CH_2CH_3), 1.54 (s, 4 H, $2H_2O$), 1.48 (t, J = 7 Hz, 12 H, CH_2CH_3) ppm.

The trimeric product was recrystallised to obtain a red solid (10.5 mg, 1 %), m.p. > 350 °C, (from CH_2Cl_2/MeOH): FAB MS: m/z = $[M + 6H]^+$ 3078.24 (calcd. 3079.28), $[M - M/3 + 4H]^+$ 2051.9 (calcd. 2052.85), $[M/3 + 2H]^+$ 1026.0 (calcd. 1026.43). UV ($CHCl_3$): λ = 411, 541, 576 nm. ^{1}H NMR (300 MHz, $CDCl_3$, 25 °C): δ = 10.09 (s, 2 H, *meso*-H), 7.76 (t, J = 8 Hz, 2 H, Ar-H), 7.73 (d, J = 7 Hz, 2 H, Ar-H), 7.34 (t, J = 7 Hz, 2 H, Ar-H), 7.28 (d, J = 8 Hz, 2 H, Ar-H), 6.39 (d, J = 8 Hz, 2 H, Ar-H), 5.17 (t, J = 8 Hz, 2 H, Ar-H), 4.11 (t, J = 4 Hz, 4 H, OCH_2), 3.93 (q, J = 7 Hz, 8 H, CH_2CH_3), 3.79 (d, J = 8 Hz, 2 H, Ar-H), 3.04 (t, J = 4 Hz, 4 H, OCH_2), 2.51 (s, 12 H, CH_3), 2.33 (t, J = 4 Hz, 4 H, OCH_2), 1.88 (t, J = 4 Hz, 4 H, OCH_2), 1.67 (t, J = 7 Hz, 12 H, CH_2CH_3) ppm.

Zinc Naphthoquinol-Strapped Porphyrin [2]Catenane 16: Naphthoquinol-strapped zincporphyrin **10b** (92 mg, 8.96×10^{-5} mol), 1,1′-[1,4-phenylenebis(methylene)]bis(4,4′-bipyridinium) bis(hexafluorophosphate) (**13**) (76 mg, 1.08×10^{-4} mol), 1,4-bis(bromomethyl)-benzene (35 mg, 1.34×10^{-4} mol), and catalytic amounts of NaI and NH_4PF_6 were stirred at room temperature in DMF (2 mL) for 14 days. The solvent was then removed under vacuum with heating, and the residue was washed well with CH_2Cl_2, followed by hot H_2O. Purification was carried out by column chromatography (silica) by eluting initially with MeOH, followed by MeOH/2 M NH_4Cl solution/$MeNO_2$ (7:2:1, v/v). The product fractions were taken to dryness, the residue dissolved in a minimum amount of MeOH/H_2O, and a solution of $Zn(OAc)_2$ in MeOH/H_2O added and allowed to stir at room temperature for one hour. The solution was then filtered and saturated NH_4PF_6 solution added to the filtrate until no further precipitation was evident. The catenane product was collected by filtration, washed (H_2O), and pumped dry. The product was recrystallised to obtain catenane **16** as a dark purple solid (37 mg, 19 %), m.p. > 350 °C (from acetone/iPr$_2$O). $C_{99}H_{100}F_{24}N_8O_6P_4Zn{\cdot}H_2O$ (2161.17): calcd. C 55.02, H 4.76, N 5.18; found C 54.74, H 4.94, N 4.98. FAB MS: m/z = $[M - PF_6^-]^+$ 1981.3 (calcd. 1979.6), $[M - 2PF_6^-]^+$ 1835.2 (calcd. 1834.6), $[M - 3PF_6^-]^+$ 1689.7 (calcd. 1689.6), $[M - 4PF_6^-]^+$ 1545.1 (calcd. 1544.7), $[M -$ tetracation $- 4PF_6^-]^+$ 1023.9 (calcd. 1024.4). UV (acetone): λ = 422, 544, 580 nm. ^{1}H NMR (300 MHz, CD_3CN, 25 °C): δ = 10.02 (s, 2 H, *meso*-H), 8.50 (m, 4 H, α,α′-bipy "outside"), 8.01 (t, J = 7 Hz, 2 H, Ar-H), 7.80 (d, J = 8 Hz, 4 H, $-C_6H_4-$ "outside"), 7.74 (d, J = 8 Hz, 2 H, Ar-H), 7.67 (m, 4 H, $-C_6H_4-$ "inside"), 7.46 (d, J = 7 Hz, 2 H, Ar-H), 7.40 (d, J = 6 Hz, 2 H, α-bipy "inside"), 7.34 (d, J = 7 Hz, 2 H, Ar-H), 7.13 (d, J = 4 Hz, 2 H, β-bipy "outside"), 6.99 (d, J = 5 Hz, 2 H, β′-bipy "outside"), 6.83 (d, J = 6 Hz, 2 H, α′-bipy "inside"), 5.60 [s, 6 H, $^+NCH_2$ "outside" (4 H), Ar-H (2 H)], 5.30 (t, J = 8 Hz, 2 H, Ar-H), 5.17 (t, J = 7 Hz, 2 H, OCH_2), 5.12 (d, J = 13 Hz, 2 H, $^+NCH_2$ "inside"), 5.02 (d, J = 13 Hz, 2 H, $^+NCH_2'$ "inside"), 4.78 (d, J = 9 Hz, 2 H, OCH_2), 4.33−4.22 (m, 4 H, CH_2CH_3), 4.11−4.02 (m, 10 H, OCH_2), 3.87−3.82 (m, 4 H, CH_2CH_3), 3.64 (dd, J = 10 Hz, 4 Hz, 2 H, OCH_2), 3.39 (d, J = 5 Hz, 2 H, β′-bipy "inside"), 3.28 (d, J = 5 Hz, 2 H, β-bipy "inside"), 2.65 (s, 6 H, CH_3), 2.60 (s, 6 H, CH_3), 1.96−1.84 (m, 12 H, CH_2CH_3), 1.47 (d, J = 8 Hz, 2 H, Ar-H) ppm.

X-ray Crystallographic Study: The structure models were refined with SHELXL-97,[29] and teXsan,[30] WinGX[31] and XTAL[32] were used for analysis and graphics. In general non-hydrogen atoms were modelled with anisotropic displacement parameters and a riding atom model was used for the hydrogen atoms. The refinement residuals are defined as $R1 = \Sigma||F_o| - |F_c||/\Sigma|F_o|$ for $F_o > 2\sigma(F_o)$ and $wR2 = [\Sigma w(F_o^2 - F_c^2)^2/\Sigma(wF_c^2)^2]^{1/2}$ for all reflections, with $w = 1/[\sigma^2(F_o^2) + (AP)^2 + BP]$ where $P = (F_o^2 + 2F_c^2)/3$ where A and B are given in the crystal data below.

The single crystals obtained for **10b** were too small to provide an acceptable data set from a conventional laboratory diffarctometer. Data were obtained during commissioning studies at the ChemMatCARS facility at the Advanced Photon Source of the Argonne National Laboratory, Argonne USA. Double diamond (111) reflections were used to obtain monochromated 0.56356 Å radiation from the synchrotron source, and harmonics were eliminated with mirrors. A red prismatic crystal was attached with Exxon Paratone N, to a short length of fibre supported on a thin piece of copper wire inserted in a copper mounting pin. The pin and crystal were mounted on a unique Bruker−Kappa diffractometer equipped with a 4-chip mosaic CCD detector, and an Oxford Scientific Cryojet. Data were collected at 123(2) Kelvin with φ scans to 44.3° 2θ, and cell constants were obtained from a least-squares refinement against 1020 reflections located between 6 and 44° 2θ. The intensities of 268 standard reflections recollected at the end of the experiment changed by 7.38 % during the data collection and a correction was accordingly applied with SADABS.[33] The data integration and reduction were undertaken with SAINT and XPREP.[34]

The structure was solved by direct methods with SIR97,[35] and the asymmetric unit contains the metalloporphyrin, a solvent site modelled with a 60 % occupancy dimethylsufoxide molecule and two 20 % occupancy water oxygen atoms. Initially a fully occupied but disordered DMSO model was used for the solvent site, with the sulfur disordered over two positions related by sp^3 inversion. However this model was unsatisfactory, having very high displacement parameters for the second sulfur site relative to the oxygen site and higher refinement residuals. Accordingly this model was abandoned, and the residual peaks were treated as partial occupancy water sites. In general the non-hydrogen atoms were modelled with anisotropic displacement parameters and a riding atom model was used for the hydrogen atoms. The partially occupied carbon and oxygen sites were modelled with isotropic displacement parameters. An ORTEP[18] depiction of the molecule with 50 % displacement ellipsoids is provided in Figure 2.

Crystal Data for 10b: Model formulation $C_{65.20}H_{73.60}N_4O_8S_{1.60}Zn$, M = 1157.95, triclinic, space group $P\bar{1}$ (No. 2), a = 15.0962(13), b = 17.1660(19), c = 14.6118(17) Å, α = 113.150(4), β =

118.166(5), γ = 64.067(5)°, V = 2917.6(5) Å^3, Z = 2, crystal size 0.110 × 0.084 × 0.029 mm, colour red, habit prism, λ(synchrotron) = 0.56356 Å, μ(synchrotron) = 0.289 mm^{-1}, T(SADABS)$_{min.,max.}$ = 0.763, 1.000, 2θ$_{max.}$ = 44.30, *hkl* range −20/20, −22/22, −19/19, N = 96208, $N_{ind.}$ = 13889(R_{merge} = 0.0428), $N_{obsd.}$ = 13207[$I > 2\sigma(I)$], $N_{var.}$ = 736, residuals $R1(F)$ 0.0426, $wR2(F^2)$ 0.1171 with A = 0.06 and B = 2.255, GoF(all) = 1.098, Δρ$_{min.,max.}$ −0.918, 1.315 e$^-$ Å^{-3}.

A dark purple prismatic crystal of **7b** was attached to a thin glass fibre and mounted on a Rigaku AFC7R diffractometer employing graphite-monochromated Cu-K_α radiation generated from a Rigaku rotating anode. Cell constants were obtained from a least-squares refinement against 25 reflections located between 19.30 and 33.50° 2θ. Data were collected at 294(2) Kelvin with ω-2θ scans to 120.18° 2θ. The data processing was undertaken with the UNIX version of teXsan.[30] The intensities of 3 standard reflections measured every 150 reflections did not change significantly during the data collection. The structure by direct methods with SHELXS-86.[36] Large displacement parameters in the porphyrin strap indicate significant disorder and/or thermal motion. An ORTEP[18] depiction of the molecule with 20 % displacement ellipsoids is provided in Figure 3.

Crystal Data for 10b: $C_{66}H_{78}N_4O_{10}Zn$, M = 1152.69, monoclinic, space group: $P2_1/c$ (No. 14), a = 13.353(2), b = 34.280(6), c = 14.824(2) Å, β = 116.510(10), V = 6072.1(16) Å^3, D_c = 1.261 g cm^{-3}, Z = 4, crystal size: 0.20 × 0.10 × 0.10 mm, colour: dark purple, habit: prismatic, T = 294(2) Kelvin, λ(Cu-K_α) 1.54178 Å, μ(Cu-K_α) = 1.054 mm^{-1}, T(φ-scans)$_{min.,max.}$ = 0.855, 0.998, 2θ$_{max.}$ = 120.18, *hkl* range: 0/14, 0/38, −16/14, N = 9339, $N_{ind.}$ = 8507 (R_{merge} = 0.1208), $N_{obsd.}$ = 2901 [$I > 2\sigma(I)$], $N_{var.}$ = 726, residuals $R1(F)$ = 0.0662, $wR2(F^2)$ = 0.1750 with A = 0.03 and B = 0.0, GoF(all) = 1.159, Δρ$_{min.,max.}$ = −0.474, 0.674 e$^-$ Å^{-3}.

CCDC-216542 and -216543 contain the supplementary crystallographic data for this paper. These data can be obtained free of charge at www.ccdc.cam.ac.uk/conts/retrieving.html [or from the Cambridge Crystallographic Data Centre, 12, Union Road, Cambridge CB2 1EZ, UK; Fax: (internat.) +44-1223/336-033; E-mail: deposit@ccdc.cam.ac.uk].

Acknowledgments

Funding for part of this project by the Australian Research Council is acknowledged. Use of the ChemMatCARS Sector 15 at the Advanced Photon Source, was supported by the Australian Synchrotron Research Program, which is funded by the Commonwealth of Australia under the Major National Research Facilities Program. ChemMatCARS Sector 15 is also supported by the National Science Foundation/Department of Energy under grant numbers CHE9522232 and CHE0087817 and by the Illinois board of higher education. The Advanced Photon Source is supported by the U.S. Department of Energy, Basic Energy Sciences, Office of Science, under Contract No. W-31-109-Eng-38.

[1] A. R. Pease, J. O. Jeppesen, J. F. Stoddart, Y. Luo, C. P. Collier, J. R. Heath, *Acc. Chem. Research* **2001**, *34*, 433. J.-M. Lehn, *Angew. Chem. Int. Ed. Engl.* **1988**, *27*, 89. V. Balzani, A. Credi, M. Venturi, *Chem. Eur. J.* **2002**, *8*, 5525.

[2] V. Balzani, M. Gómez-Lopez, J. F. Stoddart, *Acc. Chem. Research* **1998**, *31*, 405. V. Balzani, A. Credi, F. M. Raymo, J. F. Stoddart, *Angew. Chem. Int. Ed.* **2000**, *39*, 3349. B. L. Feringa, *Acc. Chem. Research* **2001**, *34*, 504. J. F. Stoddart, *Chem. Aust.* **1992**, 576. J. F. Stoddart, *Acc. Chem. Research* **2001**, *34*, 410.

[3] J.-P. Sauvage, *Acc. Chem. Research* **1998**, *31*, 611.

[4] P. R. Ashton, V. Baldoni, V. Balzani, A. Credi, H. D. A. Hoffmann, M.-V. Martinez-Diaz, F. M. Raymo, J. F. Stoddart, M. Venturi, *Chem. Eur. J.* **2001**, *7*, 3482. V. Balzani, A. Credi, S. J. Langford, F. M. Raymo, J. F. Stoddart, M. Venturi, *J. Am. Chem. Soc.* **2000**, *122*, 3542. P. R. Ashton, S. E. Boyd, A. Brindle, S. J. Langford, S. Menzer, L. Perez-Garcia, J. A. Preece, F. M. Raymo, N. Spencer, J. F. Stoddart, A. J. P. White, D. J. Williams, *New J. Chem.* **1999**, *23*, 587. M. Asakawa, P. R. Ashton, V. Balzani, A. Credi, C. Hamers, G. Mattersteig, M. Montalti, A. M. Shipway, N. Spencer, J. F. Stoddart, M. S. Tolley, M. Venturi, A. J. P. White, D. J. Williams, *Angew. Chem. Int. Ed.* **1998**, *37*, 333. P. R. Ashton, J. A. Preece, J. F. Stoddart, M. S. Tolley, A. J. P. White, D. J. Williams, *Synthesis* **1994**, 1344. Z.-T. Li, P. C. Stein, J. Becher, D. Jensen, P. Mørk, N. Svenstrup, *Chem. Eur. J.* **1996**, *2*, 624. D. J. Cárdenas, A. Livoreil, J.-P. Sauvage, *J. Am. Chem. Soc.* **1996**, *118*, 11980.

[5] D. B. Amabilino, J.-P. Sauvage, *New J. Chem.* **1998**, 395. M. Linke, N. Fujita, J. C. Chambron, V. Heitz, J. P. Sauvage, *New J. Chem.* **2001**, *25*, 790. J.-C. Chambron, C. O. Dietrich-Buchecker, V. Heitz, J.-F. Nierengarten, J.-P. Sauvage, C. Pascard, J. Guilhem, *Pure Appl. Chem.* **1995**, *67*, 233. D. B. Amabilino, J.-P. Sauvage, *Chem. Commun.* **1996**, 2441. M. J. Gunter, S. M. Farquhar, *Org. Biomol. Chem.* **2003**, *1*, 3450.

[6] L. Flamigni, A. M. Talarico, S. Serroni, F. Puntoriero, M. J. Gunter, M. R. Johnston, T. P. Jeynes, *Chem. Eur. J.* **2003**, *9*, 2649.

[7] M. J. Gunter, M. R. Johnston, *J. Chem. Soc., Chem. Commun.* **1992**, 1163.

[8] M. J. Gunter, D. C. R. Hockless, M. R. Johnston, B. W. Skelton, A. H. White, *J. Am. Chem. Soc.* **1994**, *116*, 4810.

[9] M. J. Gunter, M. R. Johnston, *J. Chem. Soc., Chem. Commun.* **1994**, 829.

[10] M. J. Gunter, R. N. Warrener, *Chem. Aust.* **1997**, 25.

[11] I. Willner, E. Kaganer, E. Joselevich, H. Durr, E. David, M. J. Gunter, M. R. Johnston, *Coord. Chem. Rev.* **1998**, *171*, 261.

[12] L. Flamigni, A. M. Talarico, M. J. Gunter, M. R. Johnston, T. P. Jeynes, *New J. Chem.* **2003**, *27*, 551.

[13] M. J. Gunter, T. P. Jeynes, M. R. Johnston, P. Turner, Z. P. Chen, *J. Chem. Soc., Perkin Trans. 2* **1998**, *21*, 1945.

[14] Cs_2CO_3 was added to the reaction to aid in the formation of the this large macrocycle by a cation templating effect, the so called "cesium effect", see: G. Dijkstra, W. H. Kruizinga, R. M. Kellogg, *J. Org. Chem.* **1987**, *52*, 4230. The modification of Maruyama's procedure (A. Osuka, F. Kobayashi, K. Maruyama, *Bull. Chem. Soc. Jpn.* **1991**, *64*, 1213. A. Osuka, T. Nagata, F. Kobayashi, K. Maruyama, *J. Heterocycl. Chem.* **1990**, *27*, 1657) that was used for some previous related porphyrin synthesis was unsuccessful in this case.

[15] M. J. Gunter, S. M. Farquhar, T. P. Jeynes, *Org. Biomol. Chem.* **2003**, *1*, 4097.

[16] J. E. Redman, J. K. M. Sanders, *Org. Lett.* **2000**, *2*, 4141.

[17] Conformational interchange can occur by rotation around the C−C and C−O bonds in the strap, and not around the meso−C to phenyl bond; rotation around this bond is restricted and interconverts the two atropisomeric **6** and **7**, or **8** and **9**.

[18] C. K. Johnson, ORTEP: *ORTEPII. Report ORNL-5138*, Oak Ridge National Laboratory, Oak Ridge, Tennessee, **1976**.

[19] PLATON, A Multipurpose Crystallographic Tool, **1998**, Utrecht University, Utrecht, The Netherlands. A. L. Spek, *Acta Crystallogr., Sect. A* **1990**, *46*, C34.

[20] Some DMSO was found necessary to improve the solubility of **7b** which otherwise tended to crystallize during the course of the NMR titration experiment. For consistency, the association constants of the other porphyrin receptors were also determined in this solvent.

[21] A table of chemical shift changes and detailed rationale for the indicated structures of the complexes is given in the Supplementary Data.

[22] M. J. Gunter, M. R. Johnston, B. W. Skelton, A. H. White, *J.*

Chem. Soc., Perkin Trans. 1 **1994**, 1009. M. J. Gunter, M. R. Johnston, *J. Chem. Soc., Perkin Trans. 1* **1994**, 995.

[23] A modification of the originally reported workup procedure was found necessary to remove the unchanged cyclophane components or the tetracationic cyclophane which proved difficult to separate from the desired catenane product by chromatography alone. This involved washing the reaction residue with hot water, followed by subsequent chromatography and anion exchange.

[24] D. B. Amabilino, P. R. Ashton, C. L. Brown, E. Córdova, L. A. Godínez, T. T. Goodnow, A. E. Kaifer, S. P. Newton, M. Pietraszkiewicz, D. Philp, F. M. Raymo, A. S. Reder, M. T. Rutland, A. M. Z. Slawin, N. Spencer, J. F. Stoddart, D. J. Williams, *J. Am. Chem. Soc.* **1995**, *117*, 1271. D. B. Amabilino, P.-L. Anelli, P. R. Ashton, G. R. Brown, E. Cordova, L. A. Godinez, W. Hayes, A. E. Kaifer, D. Philp, A. M. Z. Slawin, N. Spencer, J. F. Stoddart, M. S. Tolley, D. J. Williams, *J. Am. Chem. Soc.* **1995**, *117*, 11142.

[25] H. Ryeng, A. Ghosh, *J. Am. Chem. Soc.* **2002**, *124*, 8099. A. B. Parusel, T. Wondimagegn, A. Ghosh, *J. Am. Chem. Soc.* **2000**, *122*, 6371.

[26] S. G. DiMagno, A. K. Wertsching, I. Charles, R. Ross, *J. Am. Chem. Soc.* **1995**, *117*, 8279. A. K. Wertsching, A. S. Koch, S. G. DiMagno, *J. Am. Chem. Soc.* **2001**, *123*, 3932.

[27] P. R. Ashton, R. Ballardini, V. Balzani, A. Credi, K. R. Dress, E. Ishow, C. J. Kleverlaan, O. Kocian, J. A. Preece, N. Spencer, J. F. Stoddart, M. Venturi, S. Wenger, *Chem. Eur. J.* **2000**, *6*, 3558. R. Ballardini, V. Balzani, M. T. Gandolfi, L. Prodi, M. Venturi, D. Philp, H. G. Ricketts, J. F. Stoddart, *Angew. Chem. Int. Ed. Engl.* **1993**, *32*, 1301. Y.-Z. Hu, S. H. Bossmann, D. van Loyen, O. Schwarz, H. Dürr, *Chem. Eur. J.* **1999**, *5*, 1267.

[28] P. L. Anelli, P. R. Ashton, R. Ballardini, V. Balzani, M. Delgado, M. T. Gandolfi, T. T. Goodnow, A. E. Kaifer, D. Philp, M. Pietraszkiewicz, L. Prodi, M. V. Reddington, A. M. Z. Slawin, N. Spencer, J. F. Stoddart, C. Vicent, D. J. Williams, *J. Am. Chem. Soc.* **1992**, *114*, 193.

[29] G. M. Sheldrick, SHELXL-97. *Program for crystal structure refinement.,* University of Göttingen, Germany, **1997**.

[30] teXsan for Windows and UNIX; Single Crystal Structure Analysis Software (**1985−1999**), MSC, 3200 Research Forest Drive, The Woodlands, TX 77381, USA.

[31] L. J. Farrugia, *Appl. Cryst.* **1999**, *32*, 837.

[32] Xtal3.6 System (Eds.: S. R. Hall, D. J. du Boulay, R. Olthof-Hazekamp), University of Western Australia, **1999**.

[33] G. M. Sheldrick, SADABS. Empirical absorption correction program for area detector data., University of Gottingen, Germany, **1996**. R. H. Blessing, *Acta Crystallogr., Sect. A* **1995**, *51*, 33.

[34] Bruker, XShell, Bruker Analytical X-ray Instruments Inc., Madison, Wisconsin, USA., **2000**. Bruker, SMART, SAINT and XPREP. Area detector control and data integration and reduction software., Bruker Analytical X-ray Instruments Inc., Madison, Wisconsin, USA, **1995**.

[35] A. Altomare, M. Cascarano, C. Giacovazzo, A. J. Guagliardi, *Appl. Cryst.* **1993**, *26*, 343.

[36] G. M. Sheldrick, in *Crystallographic Computing 3* (Ed.: C. K. a. R. G. G. M. Sheldrick), Oxford University Press, Oxford UK, **1985**, pp. 175.

Received August 8, 2003